Title

The casein kinases Yck1p and Yck2p act in the secretory pathway, in part, by regulating the Rab exchange factor Sec2p

Journal

Molecular Biology of the Cell, 27(4)

ISSN

1059-1524

Authors

Stalder, Danièle
Novick, Peter J

Publication Date

2016-02-15

DOI

10.1091/mbc.e15-09-0651

Peer reviewed

The casein kinases Yck1p and Yck2p act in the secretory pathway, in part, by regulating the Rab exchange factor Sec2p

Danièle Stalder and Peter J. Novick*
Department of Cellular and Molecular Medicine, University of California, San Diego, La Jolla, CA 92093

ABSTRACT **Sec2p is a guanine nucleotide exchange factor that activates Sec4p, the final Rab GTPase of the yeast secretory pathway. Sec2p is recruited to secretory vesicles by the upstream Rab Ypt32p acting in concert with phosphatidylinositol-4-phosphate (PI(4)P). Sec2p also binds to the Sec4p effector Sec15p, yet Ypt32p and Sec15p compete against each other for binding to Sec2p. We report here that the redundant casein kinases Yck1p and Yck2p phosphorylate sites within the Ypt32p/Sec15p binding region and in doing so promote binding to Sec15p and inhibit binding to Ypt32p. We show that Yck2p binds to the autoinhibitory domain of Sec2p, adjacent to the PI(4)P binding site, and that addition of PI(4)P inhibits Sec2p phosphorylation by Yck2p. Loss of Yck1p and Yck2p function leads to accumulation of an intracellular pool of the secreted glucanase Bgl2p, as well as to accumulation of Golgi-related structures in the cytoplasm. We propose that Sec2p is phosphorylated after it has been recruited to secretory vesicles and the level of PI(4)P has been reduced. This promotes Sec2p function by stimulating its interaction with Sec15p. Finally, Sec2p is dephosphorylated very late in the exocytic reaction to facilitate recycling.**

Monitoring Editor
Akihiko Nakano
RIKEN

Received: Sep 14, 2015
Revised: Dec 12, 2015
Accepted: Dec 17, 2015

INTRODUCTION

Rab GTPases are nucleotide-dependent switches that serve as master regulators of membrane traffic (Hutagalung and Novick, 2011). Each Rab recruits a specific set of effectors that, in turn, directs different steps of a vesicular transport reaction. Because effectors, by definition, bind preferentially to the GTP-bound form of a Rab, guanine nucleotide exchange factors (GEFs) that catalyze the displacement of GDP from the Rab and thereby promote binding of GTP are essential for Rab function. Controlling when and where a GEF is active will therefore define the temporal and spatial regulation of its substrate Rab and downstream effectors.

We focus here on the final stage of the secretory pathway in the budding yeast *Saccharomyces cerevisiae*. Secretory vesicles derived from the late Golgi are delivered to sites of polarized cell surface growth, such as the tip of small buds or the neck of large-budded cells, by the type V myosin Myo2p. They are then tethered to the cell cortex at these sites by the octomeric exocyst complex and finally fuse with the plasma membrane through the formation of a *trans*–soluble *N*-ethylmaleimide–sensitive factor attachment protein receptor (SNARE) complex. The Rab GTPase Sec4p controls these three steps through direct interactions of Sec4p-GTP with Myo2p, the exocyst subunit, Sec15p, and the SNARE regulator Sro7p (Guo *et al.*, 1999; Grosshans *et al.*, 2006; Jin *et al.*, 2011).

Activation of Sec4p requires the function of Sec2p, a highly efficient and specific Sec4p GEF (Walch-Solimena *et al.*, 1997). The N-terminus of Sec2p (amino acids [aa] 1–160) forms a homodimeric coiled-coil structure that catalyzes the nucleotide exchange reaction on Sec4p, whereas the remainder of Sec2p (aa 160–759) interacts with several different ligands that together determine its subcellular localization. Both Sec4p and Sec2p are highly concentrated on the surface of secretory vesicles yet exhibit no detectable association with the Golgi membranes from which these vesicles originate. The recruitment of Sec2p to secretory vesicles requires two different signals working in concert. One signal is the upstream,

This article was published online ahead of print in MBoC in Press (http://www.molbiolcell.org/cgi/doi/10.1091/mbc.E15-09-0651) on December 23, 2015.

*Address correspondence to: Peter Novick (pnovick@ucsd.edu).

Abbreviations used: ER, endoplasmic reticulum; GEF, guanine nucleotide exchange factor; GFP, green fluorescent protein; PI(4)P, phosphatidylinositol-4-phosphate; SNARE, soluble *N*-ethylmaleimide–sensitive factor attachment protein receptor.

late Golgi–associated Rab Ypt32p (Ortiz *et al.*, 2002; Medkova *et al.*, 2006). The region of Sec2p covering aa 160 to 258 binds to the GTP-bound form of Ypt32p, and this interaction is essential for Sec2p localization. We termed this recruitment mechanism a Rab GEF cascade, and there are now several analogous examples in which a GEF for one Rab is recruited by the GTP-bound form of the preceding Rab on a membrane traffic pathway (reviewed in Mizuno-Yamasaki *et al.*, 2012). Sec2p localization also requires the Golgi-associated pool of phosphatidylinositol-4-phosphate (PI(4)P) (Mizuno-Yamasaki *et al.*, 2010). This phosphoinositide binds to several polybasic patches within a region of Sec2p downstream of the Ypt32p binding site. Mutation of those polybasic sites or loss of function of the Golgi-associated phosphatidylinositol 4-kinase Pik1p blocks Sec2p recruitment to secretory vesicles.

In addition to binding to Ypt32p-GTP and PI(4)P, Sec2p also interacts with the Sec4p effector Sec15p (Medkova *et al.*, 2006). The interaction of a GEF with an effector of its substrate Rab may promote a positive feedback loop in which the GEF activates the Rab and the Rab recruits the effector, which in turn helps to recruit more of the GEF. A GEF–effector interaction could thereby lead to the formation of a metastable membrane domain marked by high concentrations of the activated Rab, its GEF, and its effector. Of importance, Sec15p binds to the same region of Sec2p that binds to Ypt32p-GTP, and the two ligands compete against one another for binding to Sec2p.

We found that the interaction of Sec2p with its two competing binding partners, Ypt32p-GTP and Sec15p, can be regulated in several ways. Increased levels of PI(4)P inhibit the binding of Sec2p to Sec15p and thus promote binding to Ypt32p-GTP (Mizuno-Yamasaki *et al.*, 2010). This may be the situation on newly formed secretory vesicles, which have a high concentration of PI(4)P. However, by the time these vesicles have been delivered to sites of polarized surface growth, the PI(4)P levels are reduced through the action of the Osh4p protein, allowing Sec15p to displace Ypt32p on Sec2p (Ling *et al.*, 2014). Phosphorylation also plays a key role in regulating the choice of binding partner. Sec2p is highly phosphorylated under normal growth conditions (Elkind *et al.*, 2000) and the phosphorylation of a patch of serines within the shared Ypt32p/Sec15p binding site promotes binding of Sec2p to Sec15p and inhibits binding to Ypt32p-GTP (Stalder *et al.*, 2013).

Striking parallels exist between the phosphoregulation of Sec2p and Rabin8, its mammalian homologue. It was reported that the phosphorylation of Rabin8 is directed by the kinase NDR1/2 and promotes binding to Sec15p (Ultanir *et al.*, 2012; Chiba *et al.*, 2013). Nonetheless, there is no consensus site (HxRxxS/T) for a yeast NDR homologue such as Cbk1 near the phosphorylated serine patch within the Ypt32p/Sec15p binding region of Sec2p (compared with Rabin8), even though it was demonstrated that Cbk1 binds to and phosphorylates Sec2p in vitro (Kurischko *et al.*, 2008). Another study showed that, in *Candida albicans*, Sec2p is phosphorylated by the cyclin-dependent kinase Cdc28p (Bishop *et al.*, 2010). However, this kinase targets Sec2p in its C-terminal region, well downstream of the Ypt32p/Sec15p binding site. Thus it appears likely that the kinase controlling the interactions of Sec2p with Ypt32p and Sec15p in *S. cerevisiae* is neither Cbk1p nor Cdc28p. For this reason, we systematically screened for a kinase that phosphorylates Sec2p within this key regulatory region.

RESULTS

The redundant casein kinases Yck1p and Yck2p phosphorylate Sec2p in vivo

To identify the kinases(s) responsible for Sec2p phosphorylation, we performed a directed genetic screen using kinase deletion strains selected from the yeast deletion library. We observed previously that Sec2p phosphorylation leads to a slightly reduced mobility of Sec2p on SDS–PAGE gels (Stalder *et al.*, 2013). To improve the detection of a phosphorylation-dependent mobility shift of Sec2p and focus on phosphorylation of sites within the Ypt32p/Sec15p binding region, we overexpressed a truncated Sec2p protein, Sec2p 1-508, on a CEN vector in various kinase deletion strains. This allele is efficiently phosphorylated in vivo (Elkind *et al.*, 2000), interacts with all known Sec2p binding partners (Medkova *et al.*, 2006; Mizuno-Yamasaki *et al.*, 2010), and functions well as the sole copy of this essential gene (Elkind *et al.*, 2000). We observed that in lysates of yeast deleted for either *YCK1* or *YCK2* but not *YCK3*, Sec2 1-508 splits into two bands, one of which has increased mobility relative to the band in the control strain (Figure 1A). To confirm that the difference in migration of the two bands is due to a difference in Sec2p phosphorylation, we purified glutathione *S*-transferase (GST)–tagged Sec2p 1-508 overexpressed from a CEN plasmid vector in wild-type (WT) and *yck1*Δ, *yck2*Δ, and *yck3*Δ mutants and treated the isolated Sec2p preparations with calf intestinal alkaline phosphatase (CIP). We then analyzed the mobility of Sec2p by SDS–PAGE (Figure 1B). After CIP treatment, the top Sec2p band from WT and *yck3*Δ strains, which is lacking in the *yck1*Δ and *yck2*Δ mutants, disappears. Note that during the purification procedure, Sec2p from WT cells was partially dephosphorylated and appeared as a double band rather than the single upper band, as observed in Figure 1A. These observations support the proposal that Sec2p is only partially phosphorylated in *yck1*Δ and *yck2*Δ mutants. To extend these findings, we analyzed the mobility of GST-tagged Sec2p 1-508 protein from a lysate of a strain deleted for the *YCK1* gene and expressing only a thermosensitive allele of *YCK2* (*yck-ts* mutant; Robinson *et al.*, 1993). We observed that in the *yck-ts* mutant, after incubation of cells at either 25 or 37°C, Sec2p appears to be almost entirely dephosphorylated (Figure 1C). To verify that Yck1p and Yck2p are also responsible for the phosphorylation of the full-length Sec2p protein (Sec2p FL), we purified GST-tagged Sec2p FL from the control strain and the *yck-ts* mutant and treated the protein with the CIP phosphatase in the presence or absence of EDTA (a known inhibitor of CIP; Figure 1D). In the control strain, Sec2p FL exhibits a smear extending from the top of the major Sec2p band. This extension disappears after CIP treatment and yet is preserved in presence of the phosphatase inhibitor EDTA. However, in the *yck-ts* strain, Sec2p FL always appears without an extension in its nonphosphorylated form. Taken together, these findings strongly support the hypothesis that the redundant Yck1p and Yck2p kinases phosphorylate Sec2p in vivo.

Yck1p and Yck2p target phosphosites within the Sec15p/Ypt32p binding region

Next we explored whether Yck1p and Yck2p target the phosphosites within the Sec15p/Ypt32p binding region that we had identified previously (aa 181–188; Stalder *et al.*, 2013). We analyzed the mobility shift of the nonphosphorylatable (S181-8A) and phosphomimetic (S181-8D/E) alleles within the context of either GST-tagged Sec2p FL or 1-508 protein overexpressed in the control strain or the *yck-ts* mutant (Figure 1E). Sec2p FL mobility was analyzed after purification on glutathione beads, whereas Sec2p 1-508 was analyzed directly from a yeast lysate. Mutation of the 181-188 phosphosites to A or D/E greatly reduced the difference in mobility of Sec2p FL or Sec2p 1-508 observed in the *yck-ts* strain relative to the WT strain. This result implies that Yck1p and Yck2p target the phosphosites between residues 181 and 188. The residual Yck1p/2p-dependent band shift of Sec2p FL observed with the 181–188 phosphosite

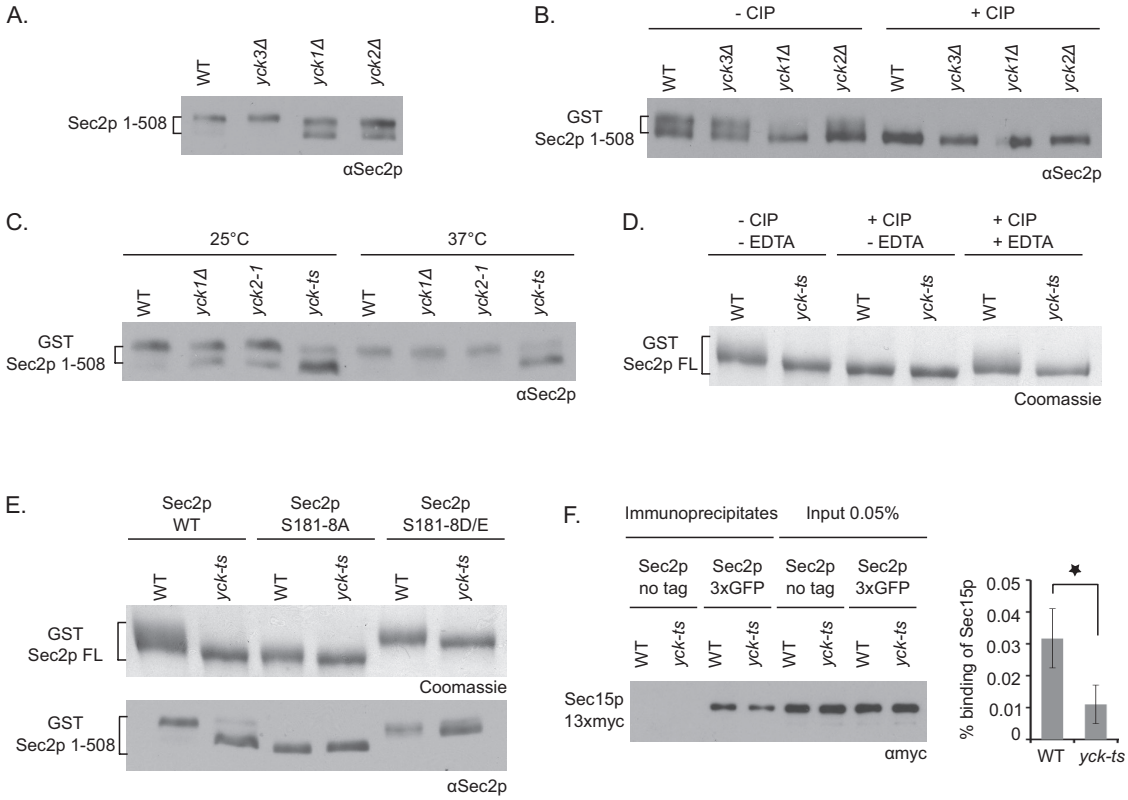

FIGURE 1: The casein kinases Yck1p and Yck2p phosphorylate Sec2p in vivo and target phosphosites within the Sec15p/Ypt32p binding region. (A) Control yeast cells or cells deleted for *YCK3*, *YCK1*, or *YCK2* genes and overexpressing Sec2p 1-508 on a CEN vector (NY3099, NY3100, NY3101, and NY3102, respectively) were grown overnight at 25°C and quickly lysed by NaOH treatment. The mobility of Sec2p 1-508 protein was visualized after SDS–PAGE gel with anti-Sec2p antibody. (B) GST–Sec2p 1-508 protein, overexpressed on a CEN vector in control yeast cells or cells deleted for *YCK3*, *YCK1*, or *YCK2* genes (NY3103, NY3104, NY3105, and NY3106, respectively), was purified, treated or not with the phosphatase CIP, and visualized after SDS–PAGE with anti-Sec2p antibody. (C) Control yeast cells, deleted for *YCK1*, expressing *yck2-1* or the *yck-ts* mutant, all overexpressing GST–Sec2p 1-508 on a CEN vector (NY3111, NY3112, NY3113, and NY3114, respectively), were grown overnight at 25°C and then shifted to 37°C for 2 h. The mobility of GST–Sec2p 1-508 protein was analyzed as in A. (D) Control yeast strain or the *yck-ts* mutant, overexpressing GST–Sec2p full length (FL) on a CEN vector (NY3115 and NY3118, respectively), were grown overnight at 25°C and then shifted to 37°C for 1 h. GST–Sec2p FL protein was purified, treated or not with the phosphatase CIP ± EDTA and visualized after SDS–PAGE by Coomassie brilliant blue staining. (E) Top, control yeast strain or the *yck-ts* mutant, overexpressing GST–Sec2p FL WT, S181-8A, or S181-8D/E on a CEN vector (NY3115, NY3118, NY3116, NY3119, NY3117, and NY3120), were grown overnight at 25°C and then shifted to 37°C for 1 h. GST Sec2p FL protein was purified and visualized after SDS–PAGE by Coomassie brilliant blue staining. Bottom, control yeast strain or the *yck-ts* mutant, overexpressing GST–Sec2p 1-508 WT, S181-8A, or S181-8D/E on a CEN vector (NY3111, NY3114, NY3121, NY3123, NY3122, and NY3124), were grown overnight at 25°C and quickly lysed by NaOH treatment. The mobility of Sec2p 1-508 protein was visualized after SDS–PAGE with anti-Sec2p antibody. (F) The Sec2p–Sec15p interaction is impaired in the *yck-ts* mutant. Sec2p-3xGFP was immunoprecipitated with GFP antibody in the control yeast strain or in the *yck-ts* mutant coexpressing Sec15p-13xmyc (NY3136 and NY3137, respectively). Yeast strains expressing untagged Sec2p (NY3134 and NY3135) were used as negative control. Coprecipitated Sec15p-13xmyc and the amount of Sec15p-13xmyc in 0.05% of lysates were detected with anti-myc antibody. The intensity of the bands was quantified using ImageJ (National Institutes of Health, Bethesda, MD). The percentage of Sec15p bound to Sec2p was calculated and indicated. Mean and SD of three different experiments. *$p < 0.03$; Student's *t* test.

mutants suggests that Yck1p/2p might also target another site in Sec2p. This residual band shift is not apparent using the Sec2p 1-508 construct, suggesting that this phosphosite resides downstream of residue 508.

Phosphomutations in Sec15p/Ypt32p binding region do not affect Sec2p GEF activity

Next we investigated whether phosphorylation within the Sec15p/Ypt32p binding region of Sec2p affects its ability to catalyze nucleotide exchange. The exchange activity of wild-type Sec2p and the nonphosphorylatable or phosphomimetic mutant (Sec2p S181-8A or D/E, respectively) was measured in vitro. Full-length GST-tagged Sec2p and the phosphosite mutants were purified from bacteria, as was full-length hexahistidine (His_6)-tagged Sec4p. Sec4p was preloaded with GDP, and then the fluorescence resonance energy transfer (FRET) signal between Sec4p tryptophans and a mant derivative of GTP was followed over time (Supplemental Figure S1). We observed that the nonphosphorylatable Sec2p (S181-8A), as

well as the phosphomimetic Sec2p (S181-8D/E), stimulated nucleotide exchange on Sec4p to a similar extent as wild-type Sec2p. This result is in line with the fact that residues 181–188 are located downstream of the catalytic coiled-coil domain (residues 1–160) of Sec2p.

The Sec2p–Sec15p interaction is impaired in the *yck-ts* mutant

Because Yck1p and Yck2p target phosphosites within the Ypt32p/Sec15p binding region, we determined whether the interaction of Sec2p with Sec15p is affected in the *yck-ts* mutant. We assessed the efficiency of coprecipitation of Sec15p-13xmyc with Sec2p-3x green fluorescent protein (GFP) from lysates of yeast expressing at endogenous levels the tagged alleles as the sole copy of each gene. After a 1-h shift of yeast cells to 37°C, Sec2p-3xGFP was immunoprecipitated with anti-GFP antibody from total lysates. Immunoprecipitates were then probed with anti-myc antibody to detect Sec15p (Figure 1F). We observed a significant threefold decrease in Sec15p–13xmyc coprecipitation in the *yck-ts* strain. We observed a similar but not statistically significant reduction when cells were incubated at 25°C rather than 37°C. These results establish that phosphorylation of Sec2p by Yck1p and Yck2p promotes the interaction of Sec2p with Sec15p.

Sec2p localization is modestly affected in a sensitized background when *YCK2* is deleted

We showed previously that locking Sec2p in either its phosphorylated or unphosphorylated state affects its localization in a sensitized background (*ypt31Δ-ypt32*^{A141D}; Stalder *et al.*, 2013). Therefore we analyzed Sec2p localization in various strains in which Yck1p and/or Yck2p are affected. In the control strain, Sec2p-3xGFP concentrates at the bud tips of small- and medium-budded cells and at the neck between the mother and bud of large-budded cells (Supplemental Figure S2A). Sec2p localization was not significantly affected in the *yck-ts* mutant either at 25°C or after a 90-min incubation at 37°C. After 90 min at 37°C, *yck-ts* mutant cells start to form elongated buds, as previously described (Robinson *et al.*, 1993). Next we analyzed Sec2p-3xGFP localization in the *ypt31Δ-ypt32*^{A141D}-sensitized background (Supplemental Figure S2B). In agreement with our prior study, in this background, the polarized localization of Sec2p-3xGFP is already affected relative to the wild-type control (compare Supplemental Figure S2, A, left, with B). However, the phenotype becomes modestly but significantly more severe when the *YCK2* gene is deleted. This result supports the idea that phosphorylation of Sec2p by Yck2p contributes to Sec2p localization, possibly by promoting a switch from binding Ypt32p-GTP to binding to Sec15p.

Sec15p and Ypt32p are not significantly mislocalized in the *yck-ts* mutant

Yck1p/Yck2p proteins are most similar at a structural level to the casein kinase 1γ (CK1γ) (Vancura *et al.*, 1994), and, accordingly, it was observed that CK1γ1 and CK1γ3 are able to complement the defects of the *yck-ts* mutant (Zhai *et al.*, 1995). Because it was reported that the *Drosophila* CK1γ homologue, gilgamesh, is important for the localization of Sec15 and Rab11 (the mammalian homologue of Ypt31p/Ypt32p; Gault *et al.*, 2012), we analyzed the localization of Sec15p-3xGFP and GFP-Ypt32p in the *yck-ts* strain. However, neither Sec15p nor Ypt32p appears to be significantly mislocalized in the mutant strain at the permissive temperature or after incubation of the cells at 37°C (Supplemental Figure S2, C and D, respectively).

Yck2p binds to the autoinhibitory region of Sec2p

Next we tested whether Yck2p is able to interact with Sec2p in vitro. Initially, we performed binding assays with N-terminally GST-tagged Sec2p and N-terminally His_6-tagged Yck2p, both expressed and purified from bacteria, but observed no detectable interaction. We considered the possibility that Yck2p might not fold efficiently in bacteria. Therefore we incubated recombinant GST-tagged Sec2p with a lysate of yeast overexpressing N-terminally GFP-tagged Yck2p. By this approach, a weak but specific interaction was detected between Yck2p and Sec2p (Figure 2B). Note that GFP-tagged Yck2p appears in two bands of differing molecular weights and that Sec2p preferentially binds to the upper band.

In a prior study, we observed that the region from amino acids 450 to 508, called the autoinhibitory region, is required for Sec2p phosphorylation in vivo (Figure 2A; Elkind *et al.*, 2000). Therefore we explored the possibility that Yck2p binds to this region. We performed binding assays of GFP-tagged Yck2p with different truncated GST-tagged Sec2p proteins. As shown in Figure 2B, Yck2p binds well to Sec2p 1-508, but the interaction with Sec2p 1-450 is almost sevenfold reduced in comparison to wild-type Sec2p. No interaction was detected with Sec2p 1-160 or GST alone. These findings indicate that the interaction of Yck2p with Sec2p requires the autoinhibitory region (aa 450–508) and are in complete agreement with our prior in vivo phosphorylation studies. Taken together, the findings support a model in which Yck2p binds to the region of Sec2p between residues 450 and 508 but then phosphorylates sites between residues 181 and 188.

Yck2p phosphorylates Sec2p in vitro

To determine whether Yck2p is able to phosphorylate Sec2p in vitro, we immunoprecipitated GFP-tagged Yck2p from a yeast lysate and incubated it with recombinant GST-tagged Sec2p 1-508 protein. We observed that in presence of wild-type Yck2p and ATP, Sec2p shifts to a higher apparent molecular weight relative to control reactions without ATP or with a dead kinase allele, Yck2p H187Y (described in Robinson *et al.*, 1993; Figure 2C). Note that the Yck2p protein appears to undergo autophosphorylation after addition of ATP. This result shows that wild-type but not kinase-dead Yck2p is able to phosphorylate Sec2p in vitro. We also observed that the S181-8A allele of Sec2p 1-508 protein undergoes less of a mobility shift upon incubation with Yck2p, supporting the hypothesis that Yck2p targets predominantly the phosphosites within the Ypt32p/Sec15p binding region.

Sec2p phosphorylation by Yck2p is inhibited by the phosphoinositide PI(4)P

We showed previously that Sec2p binds directly to the phosphoinositide PI(4)P (Mizuno-Yamasaki *et al.*, 2010). This interaction is crucial for the recruitment of Sec2p to Golgi-derived secretory vesicles and also serves to inhibit the association of Sec2p with Sec15p. We identified three positively charged patches within Sec2p that are responsible for PI(4)P binding. These patches lie just upstream and within the autoinhibitory region between residues 450 and 508 (Figure 2A). Because Yck2p binds to Sec2p near these PI(4)P binding patches, we investigated whether PI(4)P has any effect on the phosphorylation of Sec2p by Yck2p. We immunoprecipitated GFP-tagged Yck2p from a yeast lysate and incubated it with recombinant GST-tagged Sec2p 1-508 protein in the presence or absence of liposomes containing different amounts of PI(4)P. We showed previously that the truncated Sec2p 1-508 protein is able to interact with the phosphoinositide (Mizuno-Yamasaki *et al.*, 2010). We observed a dose-dependent inhibition of Sec2p phosphorylation with increasing

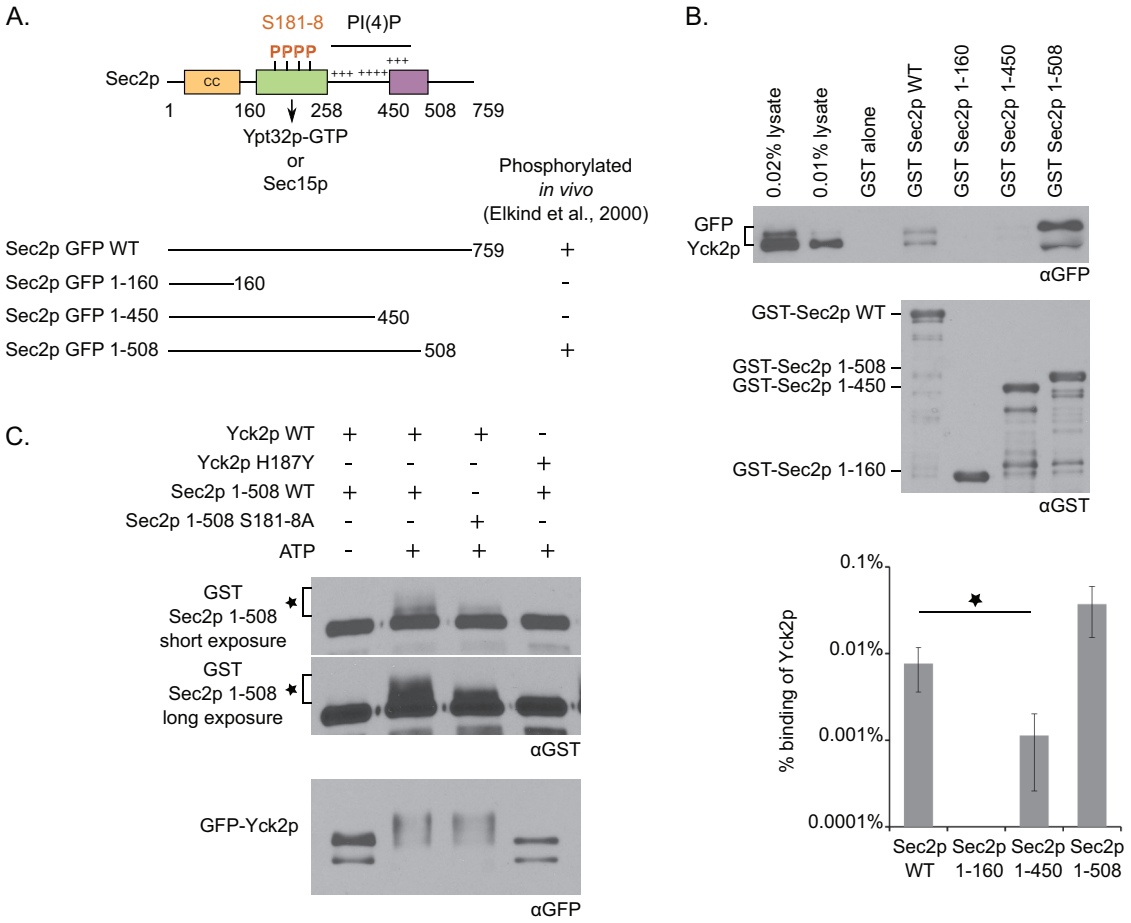

FIGURE 2: The casein kinase Yck2p binds to the autoinhibitory region of Sec2p and phosphorylates Sec2p in vitro. (A) Top, domain organization of Sec2p. The N-terminal region contains a coiled-coil domain (CC), which catalyzes the exchange of GDP for GTP on Sec4p. Downstream are overlapping binding sites for Sec15p and Ypt32p-GTP, which compete against each other to bind to Sec2p. The choice of Sec2p between these two binding partners is, in part, regulated by phosphorylation of the phosphoregion at aa 181–188. Three positively charged patches allow Sec2p to interact with the phosphoinositide PI(4)P. Finally, the region of aa 450–508, named the autoinhibitory region, negatively regulates Sec15p binding to Sec2p by an autoinhibitory mechanism. Bottom, in vivo phosphorylation results of different Sec2p constructs (Elkind *et al.*, 2000). (B) Yck2p binds to the autoinhibitory region of Sec2p. Yeast lysate overexpressing GFP-Yck2p (NY3138) was incubated with different GST-Sec2p constructs purified from bacteria and immobilized on glutathione beads. Bound GFP-Yck2p protein was detected with anti-GFP antibody. Because GST–Sec2p 1-508 protein runs at the same molecular weight as GFP-Yck2p (which explains the distortion of the GFP signal), we checked that the GFP signal is specific to GFP-Yck2p and does not cross-react with GST–Sec2p 1-508. GST-Sec2p was detected with anti-GST antibody. The intensity of the bands was quantified using ImageJ. The percentage of Yck2p bound to Sec2p was calculated and is indicated on a logarithmic scale. Mean and SD of at least three different experiments. $*p < 0.002$; Student's *t* test. The increase observed for GST–Sec2p 1-508 is not significantly different from GST–Sec2p wild type. (C) Yck2p phosphorylates Sec2p in vitro. GFP-Yck2p wild type or H187Y was immunoprecipitated from a yeast lysate with protein A/G beads (NY3138 or NY3139, respectively) and incubated with bacterial eluted GST–Sec2p 1-508 wild type or S181-8A protein. GST–Sec2p 1-508 was detected with anti-GST antibody, and the phosphorylated form is characterized by an additional band above the major Sec2p band (indicated with an asterisk). GFP-Yck2p protein was detected with anti-GFP antibody.

concentration of PI(4)P (Figure 3A). PI(4)P has no apparent effect on Yck2p activity per se, as Yck2p autophosphorylation was unaffected by increasing amounts of PI(4)P in the reaction. These results strongly suggest that the interaction of Sec2p with PI(4)P inhibits its phosphorylation by Yck2p.

Sec2p phosphorylation is affected in Pik1p and Sac1p mutants

We next investigated Sec2p phosphorylation in several yeast strains that affect the synthesis, turnover, or intracellular distribution of PI(4)P. We reported previously that in the *pik1-101* mutant (a thermosensitive allele of Pik1p), where the Golgi pool of PI(4)P is greatly reduced (Baird *et al.*, 2008), Sec2p is no longer recruited to secretory vesicles (Mizuno-Yamasaki *et al.*, 2010). In addition, in a strain deleted for *OSH4* (*osh4*Δ), we observed an accumulation of PI(4)P on secretory vesicles (Ling *et al.*, 2014). Finally, in a strain deleted for *SAC1* (*sac1*Δ), coding for a primarily endoplasmic reticulum (ER)–associated PI(4)P phosphatase, a general increase in PI(4)P level was reported (Stock *et al.*, 1999). Therefore we analyzed the mobility of GST-tagged Sec2p 1-508 from *pik1-101*, *osh4*Δ, and *sac1*Δ mutants.

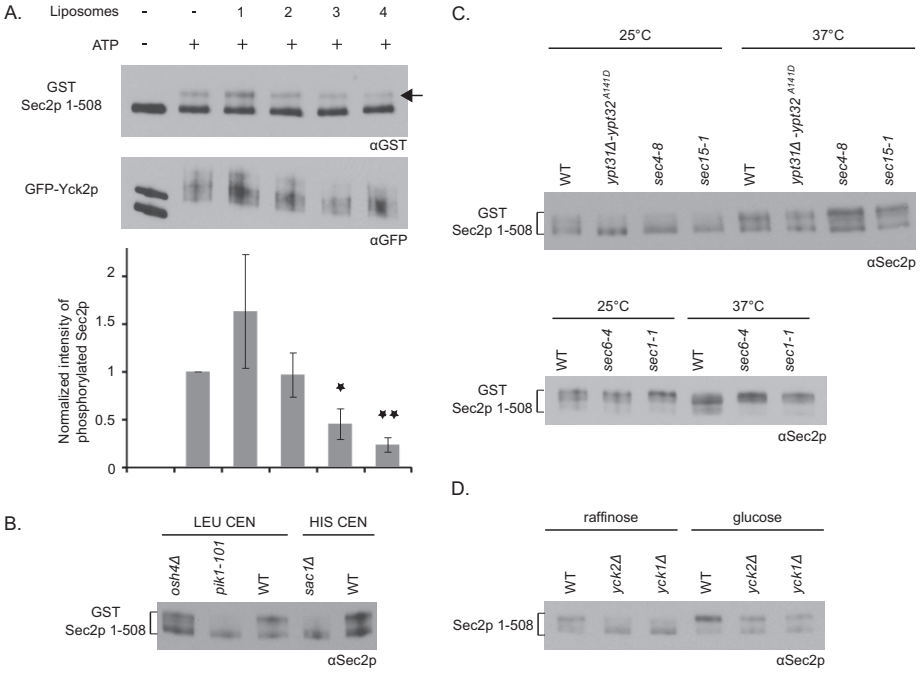

FIGURE 3: Modulation of Sec2p phosphorylation. (A) Sec2p in vitro phosphorylation by Yck2p is inhibited by the phosphoinositide PI(4)P. GFP-Yck2p was immunoprecipitated from a yeast lysate with protein A/G beads (NY3138) and incubated with bacterial eluted GST–Sec2p 1-508 and with or without ATP and liposomes containing different amounts of PI(4)P (liposomes 1–4, which contain, respectively, 0, 2, 5, and 10% PI(4)P). GST–Sec2p 1-508 was detected with anti-GST antibody, and the phosphorylated form is indicated with an arrow. GFP-Yck2p protein was detected with anti-GFP antibody. The intensity of the phosphorylated form of GST–Sec2p 1-508 was quantified using ImageJ and normalized and is indicated. Mean and SD of three different experiments. *$p < 0.03$, **$p < 0.004$; Student's *t* test relative to the condition "+ATP" (lane 2). (B) Sec2p phosphorylation is affected in Pik1p and Sac1p mutants. Control yeast cells (NY3125 and NY3103), deleted for *OSH4* (NY3132) or *SAC1* (NY3164) genes or the *pik1-101* mutant (NY3133), all overexpressing GST–Sec2p 1-508 on a CEN vector (with LEU or HIS selection), were grown overnight at 25°C and quickly lysed by NaOH treatment. The mobility of GST–Sec2p 1-508 protein was visualized after SDS–PAGE with anti-Sec2p antibody. (C) Sec2p phosphorylation may be linked to the vesicle cycle. Control yeast cells (NY3125) or *ypt31Δ-ypt32*^{A141D} (NY3126), *sec4-8* (NY3127), *sec15-1* (NY3128), *sec6-4* (NY3129), and *sec1-1* (NY3130) mutants, all overexpressing GST–Sec2p 1-508 on a CEN vector, were grown overnight at 25°C and shifted for 1 h at 37°C. Yeast cells were quickly lysed by NaOH treatment, and the mobility of GST–Sec2p 1-508 protein was visualized after SDS–PAGE with anti-Sec2p antibody. (D) Sec2p phosphorylation is stimulated in presence of glucose. Control yeast cells or cells deleted for the *YCK2* or *YCK1* genes and overexpressing Sec2p 1-508 on a CEN vector (NY3099, NY3102, and NY3101, respectively) were grown overnight at 25°C in a YP medium containing 2% raffinose and shifted for 1 h in 2% glucose. The cells were quickly lysed by NaOH treatment, and the mobility of Sec2p 1-508 protein was visualized after SDS–PAGE with anti-Sec2p antibody.

We observed reduced phosphorylation of Sec2p in *pik1-101* and *sac1*Δ lysates, whereas Sec2p phosphorylation was not significantly affected in *osh4*Δ lysates (Figure 3B). One interpretation of these results is that Sec2p must be recruited to secretory vesicles to be phosphorylated. This is consistent with the observation that Yck1p and Yck2p are lipid-modified kinases that ride on secretory vesicles to reach the plasma membrane (Babu *et al.*, 2002). Results shown in Figure 3A predict that after Sec2p recruitment, the high level of PI(4)P on immature secretory vesicles would prevent Sec2p phosphorylation by Yck1p/Yck2p until the level of PI(4)P is reduced through the action of Osh4p. We were not able to detect a significant decrease in Sec2p phosphorylation in the *osh4*Δ strain relative to wild type. Perhaps the PI(4)P on secretory vesicles in *osh4*Δ cells does not reach the level needed to strongly inhibit Sec2p phosphorylation. However, loss of Sac1p leads to a much larger increase in PI(4)P levels, and Sec2p phosphorylation was greatly reduced in this mutant.

Sec2p phosphorylation may be linked to vesicle cycle

In our previous study, we proposed that Sec2p undergoes a phosphorylation–dephosphorylation cycle that is coupled to vesicular traffic (Stalder *et al.*, 2013). By this proposal, Sec2p phosphorylation would begin once the level of PI(4)P decreases on the secretory vesicle, and dephosphorylation would occur before vesicle fusion with the plasma membrane (see later discussion of Figure 5). Therefore we analyzed the mobility of GST-tagged Sec2p 1-508 from yeast lysates expressing thermosensitive alleles of various components involved in the late stages of the secretory pathway. Figure 3C shows that, in mutants affected at an early step of the post-Golgi secretory pathway (*ypt31Δ-ypt32*^{A141D}, *sec4-8*, and *sec15-1* strains), Sec2p is predominantly unphosphorylated, as in *pik1-101*, after growth of yeast cells overnight at 25°C. We were not able to observe any difference after incubation of cells at 37°C, which stimulates phosphorylation and might thereby mask the differences in Sec2p phosphorylation. In contrast, in mutants affected in the final steps of the secretory pathway, such as *sec6-4*, defective at the tethering step, and *sec1-1*, at the fusion step (Donovan and Bretscher, 2015), Sec2p is hyperphosphorylated after incubation of cells at 37°C. This supports the hypothesis that the Sec2p phosphocycle is linked to the vesicle cycle.

Sec2p phosphorylation is stimulated in the presence of glucose

Several studies implicated Yck1p and Yck2p in glucose sensing (Estrada *et al.*, 1996; Moriya and Johnston, 2004; Gadura *et al.*, 2006). To investigate whether Sec2p phosphorylation is modulated by glucose level, we analyzed Sec2p mobility shift by SDS–PAGE of yeast lysates overexpressing Sec2p 1-508 after overnight incubation in a medium containing 2% raffinose or after 1-h shift to 2% glucose (Figure 3D). In 2% glucose, as shown in Figure 1A, Sec2p 1-508 is predominantly phosphorylated in a wild-type strain and half phosphorylated/half dephosphorylated in *yck1*Δ and *yck2*Δ mutants. However, we observed that the incubation of yeast cells in 2% raffinose leads to a shift toward the dephosphorylated form of Sec2p. These findings indicate that glucose promotes Sec2p phosphorylation.

Yck1p and Yck2p are important for efficient secretion

The Robinson laboratory showed that Yck2p rides on secretory vesicles to reach the plasma membrane (Babu *et al.*, 2002). This observation is consistent with a role for the Yck1p/Yck2p kinases in Sec2p phosphorylation. Given that we reported that Sec2p phosphorylation is important to ensure efficient vesicular transport

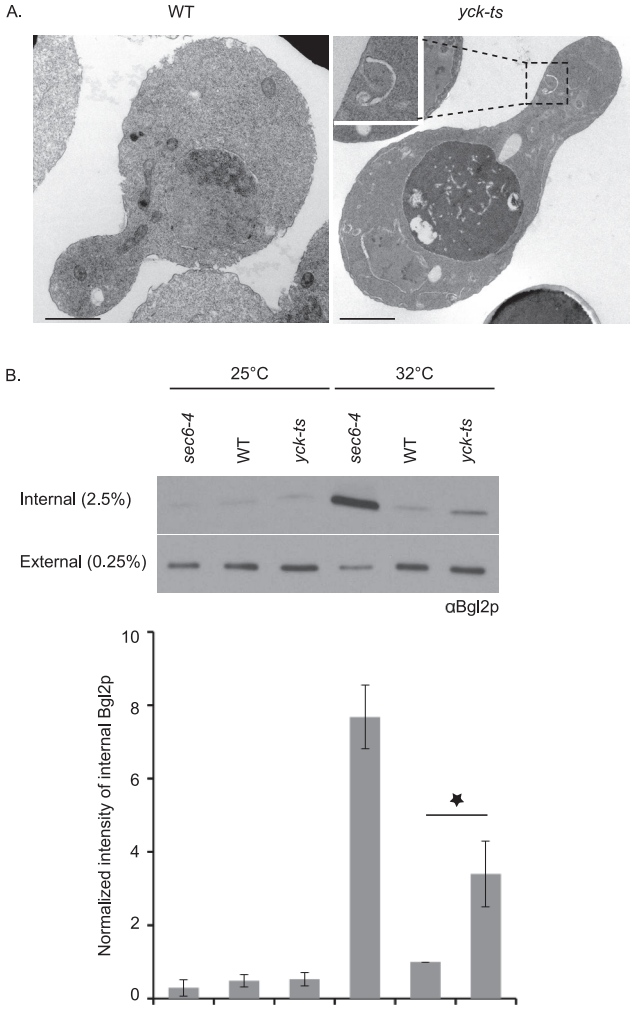

FIGURE 4: The secretory pathway is affected in the *yck-ts* strain. (A) Control yeast strain or the *yck-ts* strain (NY3109 and NY3110, respectively) were shifted at early log phase for 2 h to 37°C and processed for thin-section electron microscopy (scale bar, 1 μm). (B) Bgl2p secretion is affected in the *yck-ts* strain. Control yeast strain, the *yck-ts* mutant, and *sec6-4* strain (NY3109, NY3110, and NY17, respectively) were grown overnight at 25°C to early log phase and shifted for 1½ h to 32°C. Protein lysates from the internal and the external pool were prepared, and Bgl2p protein was detected with anti-Bgl2p antibody. The intensity of the internal Bgl2p was quantified using ImageJ and normalized (the condition WT at 32°C was set at 1) and is indicated. Mean and SD of at least three different experiments. *$p < 0.004$; Student's *t* test.

(Stalder *et al.*, 2013), we investigated the extent to which Yck1p and Yck2p are important for secretion.

First, we incubated the *yck-ts* mutant for 2 h at 37°C and examined it by thin-section electron microscopy. Compared to the wild-type strain, *yck-ts* cells accumulate several (~2.3 per cell section) Berkley bodies, aberrant Golgi-related structures not present in the control strain (Figure 4A). In addition, we often observed accumulation of debris in the vacuole. We repeated the experiment after a shift of the cells for 90 min to 32°C, to be consistent with the Bgl2p secretion experiment described later, and we again observed a Berkley body phenotype, albeit to a lesser extent (Supplemental Figure S3).

Next we analyzed the secretion of the cell wall glucanase Bgl2p in the *yck-ts* mutant (Figure 4B). We observed that, after incubation of yeast cells for 90 min at 32°C, the *yck-ts* mutant showed a threefold internal accumulation of Bgl2p protein compared with the wild-type strain. We used 32°C as the restrictive temperature for these experiments because the isogenic wild-type strain exhibited elevated internal levels of Bgl2p at 37°C. The *sec6-4* mutant, used as a bona fide secretory mutant control, accumulated a much greater fraction of Bgl2p in an intracellular pool. We also attempted to analyze the secretion of invertase in the *yck-ts* mutant, but since Yck1p/Yck2p are important for glucose sensing, and invertase repression requires this signaling pathway, the experiment could not be performed due to a failure to initially repress invertase synthesis.

We also analyzed Bgl2p secretion in yeast cells expressing Sec2p phosphomutants Sec2p S181-8A and D/E. However, we detected no Bgl2p accumulation (Supplemental Figure S4A). Finally, we investigated whether the phosphomimetic Sec2p mutant (S181-8D/E) is able to rescue the Bgl2p accumulation observed in the *yck-ts* mutant. However, Bgl2p accumulated to a similar extent in a *yck-ts* mutant expressing the phosphomimetic *SEC2* gene (Supplemental Figure S4B). Together these results strongly suggest that Yck1/2p has additional target(s) other than Sec2p, which act upstream on the secretory pathway.

Genetic interactions between *yck2* and components of the secretory machinery

Next we examined the genetic interactions between *yck2* and different components of the secretory pathway. We generated a yeast strain deleted for *YCK2* gene (in our genetic background) and crossed it to different mutant strains affected in components involved at various stages of the secretory pathway (Table 1). Dissection plates and growth test results are shown in Supplemental Figures S5 and S6, respectively. *yck2*Δ exhibits strong genetic interactions with *sec2-59* and *sec15-1* alleles, as indicated by the synthetic negative effect on growth observed at all temperatures tested. This is consistent with a stimulatory role for Yck2p in the regulation of the Sec2p–Sec15p interaction. We also observed a strong negative genetic interaction with the *pik1-101* allele on the dissection plate. Milder genetic interactions were observed with *sec12-4*, *ypt31*Δ*-ypt32*^{A141D}, *sec4-8*, *sec6-4*, *sec3-2*, *sec8-9*, *sec5-24*, *sec10-2*, and *sec1-1* alleles, since a growth defect or lethality (*sec5-24*) was observed only at 16, 30, or 33°C. No synthetic effects were observed with *sec7-1*, *sec14-3*, *gyp1*Δ, and *sec9-4* alleles. Taken together, these findings strongly suggest that the kinases Yck1/2p play an active role at one or more stages of the secretory pathway.

For comparison, we examined the genetic interactions between the nonphosphorylatable *sec2* mutant and the different components of the secretory pathway. We used a yeast strain expressing *sec2 S181-8A 3xGFP* as the only copy of *SEC2*, as well as the control strain expressing *wild-type SEC2-3xGFP*, and we crossed them to the different mutant strains (Table 2). Dissection plates and growth test results are shown in Supplemental Figures S7 and S8, respectively. We were unable to test the interaction with *sec14-3*, *gyp1*Δ, and *sec10-2* because of the lack in our collection of a strain with the appropriate selection marker. Owing to tight linkage of *SEC2* and *PIK1*, we failed to obtain double mutants in a cross with the *pik1-101* allele. We observed a strong genetic interaction of *sec2 S181-8A* with *ypt31*Δ*-ypt32*^{A141D} at all temperatures tested (Stalder *et al.*, 2013) and a mild genetic interaction with *sec3-2* at 16°C. However, we observed no synthetic effects with the other secretory components. These results strengthen the hypothesis that Yck1/2p has targets in addition to Sec2p on the secretory pathway.

Mutant	16°C	25°C	30°C	33°C
WT	No effect	No effect	No effect	No effect
sec12-4	[a]	No effect	Synthetic sick	
sec7-1	No effect	No effect	No effect	No effect
sec14-3	No effect	No effect	No effect	No effect
pik1-101	[b]	Synthetic sick[b]	[b]	[b]
gyp1Δ	No effect	No effect	No effect	No effect
ypt31Δ-ypt32^{A141D}	Synthetic sick	No effect	No effect	Synthetic sick
sec2-59	[a]	Synthetic sick	Synthetic sick	
sec4-8	Synthetic sick	No effect	No effect	
sec15-1	Synthetic sick	Synthetic sick	Synthetic sick	Synthetic sick
sec6-4	No effect	No effect	No effect	Synthetic sick
sec3-2	Synthetic sick	No effect	No effect	No effect
sec8-9	Synthetic sick	No effect	No effect	Synthetic sick
sec5-24	No effect	No effect	No effect	Synthetic lethal
sec10-2	Synthetic sick	No effect	No effect	Synthetic sick
sec1-1	Synthetic sick	No effect	No effect	Synthetic sick
sec9-4	No effect	No effect	No effect	

[a]Variability unlinked to *yck2*.

[b]We observed a strong negative genetic interaction between *yck2* and *pik1-101* on the dissection plate (Supplemental Figure S2A). However, when single mutant (*pik1-101*) or double mutants (*pik1-101+ yck2Δ*) were tested for growth, we observed variations between colonies at all indicated temperatures.

TABLE 1: Genetic interactions between *yck2* and different components of the secretory pathway.

DISCUSSION

We show here that Sec2p is subject to phosphorylation by the redundant casein kinases Yck1p and Yck2p. This modification promotes the interaction of Sec2p with the downstream effector Sec15p and contributes to Sec2p localization and function. Phosphorylation appears to be coupled to the cycle of vesicular traffic, requiring prior association of Sec2p with the vesicle and subsequent reduction of the inhibitory Golgi lipid PI(4)P from the vesicle membrane (see Figure 5 for a working model of the role of Yck1p/Yck2p's in Sec2p phosphoregulation). Dephosphorylation of Sec2p is a very late event in the transport reaction; however, it is not clear whether it normally occurs before or after exocytic fusion. A phosphomimetic *sec2* allele displays localization defects and synthetic genetic interactions that imply an important role for the dephosphorylated form of Sec2p (Stalder *et al.*, 2013), perhaps in recycling to newly formed vesicles. Although Sec2p is predominantly in its phosphorylated state under normal growth conditions, growth in a poor carbon source leads to reduced phosphorylation, consistent with a role for Yck1/2p in modulating the function of the secretory pathway in response to nutritional cues. Conversely, an increase in temperature leads to an increase in Sec2p phosphorylation, paralleling the increased growth rate at elevated temperatures. Finally, this study suggests that Yck1/2p not only regulates Sec2p but also has one or more additional targets on the secretory pathway that remain to be identified.

Yeast express four different members of the CK1 family: Yck1p, Yck2p, Yck3p, and Hrr25p. Yck1p and Yck2p were previously implicated in the regulation of endocytosis of cell surface proteins (Panek *et al.*, 1997; Marchal *et al.*, 2002; Moriya and Johnston, 2004; Gadura *et al.*, 2006). Yck3p regulates traffic to the yeast vacuole by phosphorylating the homotypic fusion and vacuole protein sorting tethering complex and the GEF Mon1 (Cabrera *et al.*, 2010; Zick and Wickner, 2012; Lawrence *et al.*, 2014), whereas Hrr25p phosphorylates the COPII coat complex directing traffic from the ER to the Golgi and also plays a key role in the regulation of autophagy (Lord *et al.*, 2011; Mochida *et al.*, 2014; Pfaffenwimmer *et al.*, 2014; Tanaka *et al.*, 2014; Wang *et al.*, 2015a). Our data implicating Yck1p and Yck2p in the regulation of traffic at the final stage of the secretory pathway fit well with this broad pattern in which all members of the CK1 kinase family act in the regulation of membrane traffic. Recent evidence shows that Hrr25p functions as an effector of the Rab GTPase Ypt1p (Wang *et al.*, 2015a). We considered that Yck1/2p might by analogy serve as an effector of either Ypt31/32p or Sec4p but found no evidence to support this (unpublished data).

The buildup of an internal pool of the cell wall glucanase Bgl2p in the *yck-ts* mutant is consistent with the proposed role of Yck1/2p in the function of Sec2p at the final stage of the secretory pathway. However, the accumulation of Golgi-related Berkley bodies rather than secretory vesicles implies an additional role for Yck1/2p within the Golgi, upstream of Sec2p function. We observed strong synthetic interactions between *yck2* and the Golgi phosphatidylinositol 4-kinase *pik1*. In addition, it was reported that, in the absence of glucose, Pik1p relocates from the *trans*-Golgi to the nucleus, possibly a manifestation of the role of Yck1/2p in glucose signaling. Furthermore in vitro kinase assays showed that Yck2p can phosphorylate Pik1p (Ptacek *et al.*, 2005; Demmel *et al.*, 2008), and four of the known phosphosites (www.phosphogrid.org/sites/35573) within the Pik1p sequence fit the consensus for casein kinases. Therefore it is possible that the proposed role for Yck1/2p in Golgi function reflects the phosphorylation of Pik1p by Yck1/2p. Nonetheless, the putative Golgi target of Yck1/2p has not yet been established.

Homologues of Sec2p in other species are also regulated by phosphorylation. The mammalian homologue Rabin8 is phosphorylated at a site that aligns closely with the Yck1/2p site in Sec2p, residues 181–188 (S272 present in the consensus site HxRxxS/T; Ultanir *et al.*, 2012; Chiba *et al.*, 2013; Supplemental Figure S9). Phosphorylation at this site promotes interaction with the mammalian

Mutant	16°C	25°C	30°C	32/33°C
WT	No effect[a]	No effect[a]	No effect[a]	No effect[a]
sec12-4	[b]	No effect	No effect	
ypt31Δ-ypt32^{A141D}	Synthetic sick[a]	Synthetic sick[a]	Synthetic sick[a]	Synthetic sick[a]
sec4-8	No effect	No effect	No effect	
sec15-1	No effect	No effect	No effect	No effect
sec6-4	No effect	No effect	No effect	No effect
sec3-2	Synthetic sick	No effect	No effect	No effect
sec8-9	No effect	No effect	No effect	No effect
sec5-24	No effect	No effect	No effect	[b]
sec1-1	No effect	No effect	No effect	No effect
sec9-4	No effect	No effect	No effect	

[a]See Stalder *et al.* (2013).
[b]Variability unlinked to *sec2 S181-8A 3xGFP*.

TABLE 2: Genetic interactions between *sec2 S181-8A 3xGFP* and different components of the secretory pathway.

homologue of Sec15p, whereas blocking phosphorylation impairs the role of Rabin8 in ciliogenesis and dendritic spine development. Nonetheless, phosphorylation in this situation is mediated by the NDR1/2 kinase, not a casein kinase. The yeast genome encodes three homologues of the NDR kinase family: Cbk1p, Dbf2p, and Dbf20p (Hergovich *et al.*, 2006). The 181–188 site does not fit the consensus for this class of kinase, which has a preference for basic amino acids (Mazanka *et al.*, 2008). Furthermore, Sec2p 1-508 phosphorylation is unaffected in a drug-sensitive Cbk1 mutant (Cbk1-as) or in strains deleted for *DBF2* or *DBF20* (unpublished data). Rabin8 is phosphorylated by the ERK1/2 kinase at four sites (SP motifs; two of which, S247 and S250, are indicated in Supplemental Figure S9) that lie upstream of the region aligning with residues 181–188 in Sec2p (Wang *et al.*, 2015b). Unlike phosphorylation by NDR2 (Chiba *et al.*, 2013), phosphorylation by ERK1/2 stimulates the exchange activity of Rabin8 by relieving autoinhibition (Wang *et al.*, 2015b). Our results indicate that phosphorylation in the Sec15p/Ypt32p binding region does not affect the exchange activity of Sec2p, excluding such a mechanism, at least for these phosphosites (S181–188); instead, they are more important for the localization of Sec2p and its interaction with binding partners.

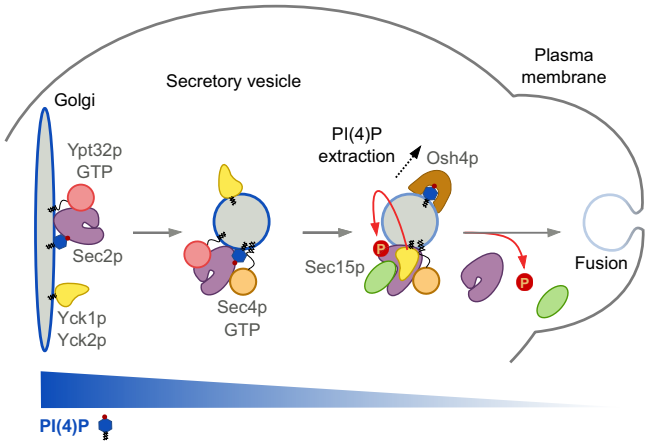

FIGURE 5: Model for Yck1p/Yck2p's role in Sec2p phosphoregulation. Nonphosphorylated Sec2p is recruited to the Golgi by the recognition of both the Rab Ypt32p-GTP and the phosphoinositide PI(4)P. Once recruited to membranes, Sec2p phosphorylation by the kinases Yck1p/Yck2p, which uses the secretory pathway to reach the plasma membrane, is inhibited by the high level of PI(4)P. The Golgi-derived secretory vesicle buds off, and Sec2p activates the Rab Sec4p, which recruits its effector, Sec15p. During the transit of the vesicle to the cell surface, the PI(4)P level drops by the action of the lipid transporter Osh4p. This triggers a conformation change in Sec2p, allowing Sec15p to replace Ypt32p-GTP on Sec2p, and allows Sec2p phosphorylation by Yck1p/Yck2p, which further enhances the Sec2p–Sec15p interaction. This process pushes the reaction forward and creates a positive-feedback loop that generates a microdomain of high Sec4p-GTP and Sec15p, facilitating the delivery, tethering, and fusion of the vesicle with the plasma membrane. Before fusion, Sec2p is dephosphorylated by a yet-unknown phosphatase that allows Sec2p to dissociate from Sec15p and thus dissociate from the vesicle. The unphosphorylated Sec2p is then ready to associate with a new round of secretory vesicles and thus ensure the continuity of vesicular transport.

As master regulators of membrane traffic, Rab GTPases must themselves be subject to regulation. Rab GEFs represent key focal points of regulation by different signaling pathways. Whereas different pathways are used in different species and perhaps in different tissues, many of the underlying regulatory mechanisms are well conserved.

MATERIALS AND METHODS

Plasmid construction and strains

Lists of *S. cerevisiae* strains and plasmids used in this study and their genotypes are given in Table 3 and Supplemental Tables S1 and S2. All vectors generated in this study were checked by sequencing.

To generate the p415 GPDp GST Sec2 1-508 CEN vector (LEU) (NRB1601), the GST Sec2 1-508 fragment was excised from NRB1156 with *Pst*1 and *Hin*dIII and cloned back into NRB851.

To generate the p413 GPDp Sec2 1-508 CEN vector (HIS; NRB1599), the Sec2 1-508 fragment was excised from the p415 GPDp GST Sec2 1-508 CEN vector (NRB1601) with *Bam*H1 and *Sal*1 and cloned back into NRB847.

To generate the p413 GPDp GST Sec2 1-508 CEN vector (HIS; NRB1600), the GST Sec2 1-508 fragment was excised from the p415 GPDp GST Sec2 1-508 CEN vector (LEU; (NRB1601) with *Spe*1 and *Sal*1 and cloned back into NRB847.

To generate p415 GPDp GST Sec2 1-508 S181-8A or D/E CEN vectors (LEU; (NRB1605 and NRB1606, respectively), Sec2

Yeast name	Alias	Background/ parental strain	Genotype	Source
NY3099	DSY157	BY4741	MATa, his3Δ1 leu2Δ0 met15Δ0 ura3Δ0 [p413 GPDp Sec2 1-508, CEN HIS]	This study
NY3100	DSY153	BY4741	MATa, his3Δ1 leu2Δ0 met15Δ0 ura3Δ0 [Δyck3::KanMX4] [p413 GPDp Sec2 1-508, CEN HIS]	This study
NY3101	DSY154	BY4741	MATa, his3Δ1 leu2Δ0 met15Δ0 ura3Δ0 [Δyck1::KanMX4] [p413 GPDp Sec2 1-508, CEN HIS]	This study
NY3102	DSY155	BY4741	MATa, his3Δ1 leu2Δ0 met15Δ0 ura3Δ0 [Δyck2::KanMX4] [p413 GPDp Sec2 1-508, CEN HIS]	This study
NY3103	DSY158	BY4741	MATa, his3Δ1 leu2Δ0 met15Δ0 ura3Δ0 [p413 GPDp GST Sec2 1-508, CEN HIS]	This study
NY3104	DSY161	BY4741	MATa, his3Δ1 leu2Δ0 met15Δ0 ura3Δ0 [Δyck3::KanMX4] [p413 GPDp GST Sec2 1-508, CEN HIS]	This study
NY3105	DSY162	BY4741	MATa, his3Δ1 leu2Δ0 met15Δ0 ura3Δ0 [Δyck1::KanMX4] [p413 GPDp GST Sec2 1-508, CEN HIS]	This study
NY3106	DSY163	BY4741	MATa, his3Δ1 leu2Δ0 met15Δ0 ura3Δ0 [Δyck2::KanMX4] [p413 GPDp GST Sec2 1-508, CEN HIS]	This study
NY3107	DSY169/LRB264	LR	MATa, his3 leu2 ura3-52 [Δyck1::URA3]	Lucy Robinson
NY3108	DSY170/LRB265	LR	MATα, his3 leu2 ura3-52 [yck2-1::HIS3]	Lucy Robinson
NY3109	DSY171/LRB341	LR	MATa, his3 leu2 ura3-52	Lucy Robinson
NY3110	DSY172/LRB345	LR	MATa, his3 leu2 ura3-52 Δyck1 yck2-2ts	Lucy Robinson
NY3111	DSY180	DSY171	MATa, his3 leu2 ura3-52 [p415 GPDp GST Sec2 1-508, CEN LEU]	This study
NY3112	DSY176	DSY169	MATa, his3 leu2 ura3-52 [Δyck1::URA3] [p415 GPDp GST Sec2 1-508, CEN LEU]	This study
NY3113	DSY178	DSY170	MATa, his3 leu2 ura3-52 [yck2-1::URA3] [p415 GPDp GST Sec2 1-508, CEN LEU]	This study
NY3114	DSY182	DSY172	MATa, his3 leu2 ura3-52 Δyck1 yck2-2ts [p415 GPDp GST Sec2 1-508, CEN LEU]	This study
NY3115	DSY320	DSY171	MATa, his3 leu2 ura3-52 [p415 GPDp GST Sec2 full-length WT, CEN LEU]	This study
NY3116	DSY322	DSY171	MATa, his3 leu2 ura3-52 [p415 GPDp GST Sec2 full-length S181A + T183A + S184A + S185A + S186A + T187A + S188A, CEN LEU]	This study
NY3117	DSY324	DSY171	MATa, his3 leu2 ura3-52 [p415 GPDp GST Sec2 full-length S181D + T183E + S184D + S185D + S186D + T187E + S188D, CEN LEU]	This study
NY3118	DSY326 DSY327	DSY172	MATa, his3 leu2 ura3-52 Δyck1 yck2-2ts [p415 GPDp GST Sec2 full-length WT, CEN LEU]	This study
NY3119	DSY329	DSY172	MATa, his3 leu2 ura3-52 Δyck1 yck2-2ts [p415 GPDp GST Sec2 full-length S181A + T183A + S184A + S185A + S186A + T187A + S188A, CEN LEU]	This study
NY3120	DSY331	DSY172	MATa, his3 leu2 ura3-52 Δyck1 yck2-2ts [p415 GPDp GST Sec2 full-length S181D + T183E + S184D + S185D + S186D + T187E + S188D, CEN LEU]	This study
NY3121	DSY209	DSY171	MATa, his3 leu2 ura3-52 [p415 GPDp GST Sec2 1-508 S181A + T183A + S184A + S185A + S186A + T187A + S188A, CEN LEU]	This study
NY3122	DSY211	DSY171	MATa, his3 leu2 ura3-52 [p415 GPDp GST Sec2 1-508 S181D + T183E + S184D + S185D + S186D + T187E + S188D, CEN LEU]	This study
NY3123	DSY213	DSY172	MATa, his3 leu2 ura3-52 Δyck1 yck2-2ts [p415 GPDp GST Sec2 1-508 S181A + T183A + S184A + S185A + S186A + T187A + S188A, CEN LEU]	This study

TABLE 3: Yeast strains.

Continues

Yeast name	Alias	Background/ parental strain	Genotype	Source
NY3124	DSY215	DSY172	MATa, his3 leu2 ura3-52 Δyck1 yck2-2ts [p415 GPDp GST Sec2 1-508 S181D + T183E + S184D + S185D + S186D + T187E + S188D, CEN LEU]	This study
NY3125	DSY130	NY1210	MATa, his3-Δ200 leu2-3112 ura3-52 GAL+ [p415 GPDp GST Sec2 1-508, CEN LEU]	This study
NY3126	DSY348	NY3039	MATα, his3-Δ200 leu2-3112 ura3-52 ypt31Δ::HIS3 ypt32A141D [p415 GPDp GST Sec2 1-508, CEN LEU]	This study
NY775			MATa, leu2-3112 sec4-8	Laboratory strain
NY3127	DSY240	NY775	MATa, leu2-3112 sec4-8 [p415 GPDp GST Sec2 1-508, CEN LEU]	This study
NY786			MATa, leu2-3112 ura3-52 sec15-1	Laboratory strain
NY3128	DSY234	NY786	MATa, leu2-3112 ura3-52 sec15-1 [p415 GPDp GST Sec2 1-508, CEN LEU]	This study
NY884			MATa, leu2-3112 ura3-52 sec6-4	Laboratory strain
NY3129	DSY236		MATa, leu2-3112 ura3-52 sec6-4 [p415 GPDp GST Sec2 1-508, CEN LEU]	This study
NY769			MATa, leu2-3112 sec1-1	Laboratory strain
NY3130	DSY237		MATa, leu2-3112 sec1-1 [p415 GPDp GST Sec2 1-508, CEN LEU]	This study
NY3131	Ling060		MATα, his3-Δ200 leu2-3112 ura3-52 GAL+ [Δosh4::KanMX4]	Laboratory strain
NY3132	DSY442	Ling060	MATα, his3-Δ200 leu2-3112 ura3-52 GAL+ [Δosh4::KanMX4] [p415 GPDp GST Sec2 1-508, CEN LEU]	This study
NY3133	DSY441	NY2187	MATα, leu2-3112 pik1-101 [p415 GPDp GST Sec2 1-508, CEN LEU]	This study
NY3134	DSY196	DSY171	MATa, his3 leu2 ura3-52 SEC15::[Sec15-13xmyc URA]	This study
NY3135	DSY198	DSY172	MATa, his3 leu2 ura3-52 Δyck1 yck2-2ts SEC15::[Sec15-13xmyc URA]	This study
NY3136	DSY204	DSY171	MATa, his3 leu2 ura3-52 SEC2::[Sec2 WT 3xGFP LEU2] SEC15::[Sec15-13xmyc URA]	This study
NY3137	DSY207	DSY172	MATa, his3 leu2 ura3-52 Δyck1 yck2-2ts SEC2::[Sec2 WT 3xGFP LEU2] SEC15::[Sec15-13xmyc URA]	This study
NY1210			MATa, his3-Δ200 leu2-3112 ura3-52 GAL+	Laboratory strain
NY3138	DSY267	NY1210	MATa, his3-Δ200 leu2-3112 ura3-52 GAL+ [YEp352 GFP Yck2, 2μ URA]	This study
NY3139	DSY337	NY1210	MATa, his3-Δ200 leu2-3112 ura3-52 GAL+ [YEp352 GFP Yck2 H187Y, 2μ URA]	This study
NY3140	DSY245	NY1210	MATa, his3-Δ200 leu2-3112 ura3-52 GAL+ [Δyck2::kanMX6]	This study
NY3039	MY481	NY1210	MATα, his3-Δ200 leu2-3112 ura3-52 [ypt31Δ::HIS3] $ypt32^{A141D}$	Laboratory strain
NY3141	DSY251	NY	His3-Δ200 leu2-3112 ura3-52 [ypt31Δ::HIS3] $ypt32^{A141D}$ [Δyck2::kanMX6]	This study
NY787		NY	MATα, leu2-3112 sec15-1	Laboratory strain
NY3142	DSY263	NY	leu2-3112 sec15-1 [Δyck2::kanMX6]	This study
NY27		NY	MATα, ura3-52 sec2-59	Laboratory strain
NY3143	DSY255	NY	ura3-52 sec2-59 [Δyck2::kanMX6]	This study
NY774		NY	MATα, leu2-3112 ura3-52 sec4-8	Laboratory strain
NY3144	DSY259	NY	leu2-3112 ura3-52 sec4-8 [Δyck2::kanMX6]	This study
NY427		RS	MATα, leu2-3112 ura3-52 trp1– his4– sec12-4	Laboratory strain
NY3145	DSY278	NY	leu2-3112 ura3-52 trp1– his4– sec12-4 [Δyck2::kanMX6]	This study

TABLE 3: Yeast strains.

Continues

Yeast name	Alias	Background/ parental strain	Genotype	Source
NY760		NY	MATα, ura3-52 sec7-1	Laboratory strain
NY3146	DSY281	NY	ura3-52 sec7-1 [Δyck2::kanMX6]	This study
NY778		NY	MATα, leu2-3112 ura3-52 sec6-4	Laboratory strain
NY3147	DSY285	NY	leu2-3112 ura3-52 sec6-4 [Δyck2::kanMX6]	This study
NY831		NY	MATα, leu2-3112 ura3-52 sec9-4	Laboratory strain
NY3148	DSY289		leu2-3112 ura3-52 sec9-4 [Δyck2::kanMX6]	This study
NY768		NY	MATα, leu2-3112 ura3-52 sec1-1	Laboratory strain
NY3149	DSY293		leu2-3112 ura3-52 sec1-1 [Δyck2::kanMX6]	This study
NY1224		NY	MATα, leu2-3112 ura3-52 sec3-2	Laboratory strain
NY3150	DSY296	NY	leu2-3112 ura3-52 sec3-2 [Δyck2::kanMX6]	This study
NY780		NY	MATα, leu2-3112 ura3-52 sec8-9	Laboratory strain
NY3151	DSY304	NY	leu2-3112 ura3-52 sec8-9 [Δyck2::kanMX6]	This study
NY776		NY	MATα, leu2-3112 ura3-52 sec5-24	Laboratory strain
NY3152	DSY300	NY	leu2-3112 ura3-52 sec5-24 [Δyck2::kanMX6]	This study
NY63		NY	MATα, his4-619 sec10-2	Laboratory strain
NY3153	DSY308	NY	his4-619 sec10-2 [Δyck2::kanMX6]	This study
NY1420			MATα, leu2-3112 sec14-3	Laboratory strain
NY3154	DSY367		leu2-3112 sec14-3 [Δyck2::kanMX6]	This study
NY2331		NY	MATα, leu2-3112 ura3-52 ade2 ade3 his3 [Δgyp1::LEU2]	Laboratory strain
NY3155	DSY363		leu2-3112 ura3-52 ade2 ade3 his3 [Δgyp1::LEU2] [Δyck2::kanMX6]	This study
NY2187		NY	MATα, leu2-3112 pik1-101	Laboratory strain
NY17		NY	MATa, ura3-52 sec6-4	Laboratory strain
NY3156	DSY184	LR	MATa, his3 leu2 ura3-52 SEC2::[Sec2-WT-3xGFP HIS3]	This study
NY3157	DSY186/188	LR	MATa, his3 leu2 ura3-52 Δyck1 yck2-2ts SEC2::[Sec2-WT-3xGFP HIS3]	This study
NY3158	DSY316	NY3039	MATα, his3-Δ200 leu2-3112 ura3-52 [ypt31Δ::HIS3] ypt32^{A141D} SEC2::[Sec2-WT-3xGFP LEU2]	This study
NY3159	DSY319	DSY251	His3-Δ200 leu2-3112 ura3-52 [ypt31Δ::HIS3] ypt32^{A141D} [Δyck2::kanMX6] SEC2::[Sec2-WT-3xGFP LEU2]	This study
NY3160	DSY273	LR	MATa, his3 leu2 ura3-52 SEC15::[Sec15-3xGFP HIS]	This study
NY3161	DSY274	LR	MATa, his3 leu2 ura3-52 Δyck1 yck2-2ts SEC15::[Sec15-3xGFP HIS]	This study
NY3162	DSY225	LR	MATa, his3 leu2 ura3-52 URA::[ADHp-GFP-Ypt32]	This study
NY3163	DSY229	LR	MATa, his3 leu2 ura3-52 Δyck1 yck2-2ts URA::[ADHp-GFP-Ypt32]	This study
NY3164	DSY437	BY4741	MATa, his3Δ1 leu2Δ0 met15Δ0 ura3Δ0 [Δsac1::KanMX4] [p413 GPDp Sec2 1-508, CEN HIS]	This study
NY2911		NY	MATa, his3-Δ200 leu2-3112 ura3-52 SEC2::[Sec2-WT-3xGFP LEU2]	Laboratory strain
NY3037		NY	MATa, his3-Δ200 leu2-3112 ura3-52 SEC2::[Sec2-S181A + T183A + S184A + S185A + S186A + T187A + S188A-3xGFP LEU2]	Laboratory strain
NY3165	DSY76	NY	leu2-3112 ura3-52 sec4-8 SEC2::[Sec2-WT-3xGFP LEU2]	This study
NY3166	DSY77	NY	leu2-3112 ura3-52 sec4-8 SEC2::[Sec2-S181A + T183A + S184A + S185A + S186A + T187A + S188A-3xGFP LEU2]	This study
NY3167	DSY475	NY	leu2-3112 sec15-1 SEC2::[Sec2-WT-3xGFP LEU2]	This study
NY3168	DSY476	NY	leu2-3112 sec15-1 SEC2::[Sec2-S181A + T183A + S184A + S185A + S186A + T187A + S188A-3xGFP LEU2]	This study
NY3169	DSY189	LR	MATa, his3 leu2 ura3-52 SEC2::[Sec2-WT-3xGFP LEU2]	This study

TABLE 3: Yeast strains.

Continues

Yeast name	Alias	Background/ parental strain	Genotype	Source
NY3170	DSY471	LR	MATa, his3 leu2 ura3-52 SEC2::[Sec2-S181A + T183A + S184A + S185A + S186A + T187A + S188A-3xGFP LEU2]	This study
NY3171	DSY465	LR	MATa, his3 leu2 ura3-52 SEC2::[Sec2-S181D + T183E + S184D + S185D + S186D + T187E + S188D-3xGFP LEU2]	This study
NY3172	DSY483	NY	leu2-3112 ura3-52 sec1-1 SEC2::[Sec2-WT-3xGFP LEU2]	This study
NY3173	DSY484	NY	leu2-3112 ura3-52 sec1-1 SEC2::[Sec2-S181A + T183A + S184A + S185A + S186A + T187A + S188A-3xGFP LEU2]	This study
NY3174	DSY494	NY	leu2-3112 ura3-52 sec3-2 SEC2::[Sec2-WT-3xGFP LEU2]	This study
NY3175	DSY495	NY	leu2-3112 ura3-52 sec3-2 SEC2::[Sec2-S181A + T183A + S184A + S185A + S186A + T187A + S188A-3xGFP LEU2]	This study
NY3176	DSY504	NY	leu2-3112 ura3-52 trp1– his4– sec12-4 SEC2::[Sec2-WT-3xGFP LEU2]	This study
NY3177	DSY505	NY	leu2-3112 ura3-52 trp1– his4– sec12-4 SEC2::[Sec2-S181A + T183A + S184A + S185A + S186A + T187A + S188A-3xGFP LEU2]	This study
NY3178	DSY192	LR	MATa, his3 leu2 ura3-52 Δyck1 yck2-2ts SEC2::[Sec2-WT-3xGFP LEU2]	This study
NY3179	DSY468	LR	MATa, his3 leu2 ura3-52 Δyck1 yck2-2ts SEC2::[Sec2-S181D + T183E + S184D + S185D + S186D + T187E + S188D-3xGFP LEU2]	This study
NY3180	DSY507	NY	leu2-3112 ura3-52 sec8-9 SEC2::[Sec2-WT-3xGFP LEU2]	This study
NY3181	DSY508	NY	leu2-3112 ura3-52 sec8-9 SEC2::[Sec2-S181A + T183A + S184A + S185A + S186A + T187A + S188A-3xGFP LEU2]	This study
NY3182	DSY515	NY	leu2-3112 ura3-52 sec6-4 SEC2::[Sec2-WT-3xGFP LEU2]	This study
NY3183	DSY516	NY	leu2-3112 ura3-52 sec6-4 SEC2::[Sec2-S181A + T183A + S184A + S185A + S186A + T187A + S188A-3xGFP LEU2]	This study
NY3184	DSY523	NY	leu2-3112 ura3-52 sec5-24 SEC2::[Sec2-WT-3xGFP LEU2]	This study
NY3185	DSY524	NY	leu2-3112 ura3-52 sec5-24 SEC2::[Sec2-S181A + T183A + S184A + S185A + S186A + T187A + S188A-3xGFP LEU2]	This study
NY3186	DSY531	NY	leu2-3112 ura3-52 sec9-4 SEC2::[Sec2-WT-3xGFP LEU2]	This study
NY3187	DSY532	NY	leu2-3112 ura3-52 sec9-4 SEC2::[Sec2-S181A + T183A + S184A + S185A + S186A + T187A + S188A-3xGFP LEU2]	This study

TABLE 3: Yeast strains. Continued

fragments bearing the mutations were excised from pGEX4T1 Sec2 vectors (NRB1498 and NRB1499, respectively; described in (Stalder *et al.*, 2013) with *Nsi*1 and *Nde*I and cloned back into the p415 GPDp GST Sec2 1-508 CEN vector (LEU; NRB1601).

To generate p415 GPDp GST Sec2 full-length WT, S181-A, or D/E CEN vectors (LEU; NRB1602, NRB1603, and NRB1604, respectively), GST Sec2 full-length fragments were excised from pNB529 GST Sec2 vectors (NRB1153, NRB1500, and NRB1501, respectively; described in Stalder *et al.*, 2013) with *Pst*1 and *Hin*dIII and cloned back into NRB851.

All of these vectors were transformed into yeast with different backgrounds to analyze Sec2p phosphorylation by mobility shift on SDS–PAGE.

To generate the GST-Sec2 1-508 S181-8A mutant for bacterial expression (NRB1610), Sec2 fragments bearing the mutations were excised from pGEX4T1-Sec2 vector (NRB1498; described in Stalder *et al.*, 2013) with *Nsi*1 and *Nde*I and cloned back into the pGEX4T1 Sec2 1-508 vector (NRB1432). This plasmid was then expressed in *Escherichia coli*, and the protein was used for the in vitro kinase assay.

The Yep352 GFP Yck2 H187Y vector (NRB1609), used for the in vitro kinase assay, was generated by PCR-based site-directed mutagenesis of the Yep352 GFP Yck2 vector (NRB1608; a gift from the Lucy Robinson laboratory, Louisiana State University Health Sciences Center, Shreveport, LA). Yep352 GFP Yck2 WT or H187Y vectors were then transformed into yeast (NY3138 and NY3139).

To generate the pRS306 Sec15C-13xmyc-ADHt vector (NY1607), the fragment 13xmyc-ADHt was excised from pRS306-Exo70C-13xmyc-ADHt (DLP78; unpublished vector) with *Bam*H1 and *Sac*1 and was used to replace the 3xGFP-ADHt fragment in the pRS306 Sec15C-3xGFP-ADHt (NRB1308). After cloning, the deletion of one nucleotide was realized by PCR-based site-directed mutagenesis between Sec15C and 13xmyc in order to have the two sequences in the same reading frame. The plasmid was then linearized using SexA1 and transformed into yeast (NY3109 and NY3110 to generate, respectively, NY3134 and NY3135) at the *SEC15* locus. The expression of Sec15-13xmyc was verified by Western blotting with anti-myc antibody (1:1000 dilution, 9B11 mouse; Cell Signaling Technology, Danvers, MA), as well as by PCR

analysis to confirm that the 13xmyc had integrated into the sole full-length copy of *SEC15* in the genome. These strains were then further transformed at the *SEC2* locus with pRS305 3xGFP-Sec2 (NRB1416) linearized with *Nsi*1. PCR analysis was performed to confirm that the 3xGFP had integrated into the sole full-length copy of *SEC2* in the genome (NY3136 and NY3137). NY3134, NY3135, NY3136, and NY3137 were then used for Sec2p–Sec15p coimmunoprecipitation assays.

To analyze Sec2p localization, the pRS303 Sec2C-3xGFP yeast integrating vector (NRB1442) was linearized using *Xba*1 and transformed into the control yeast strain or the *yck-ts* mutant at the *SEC2* locus (NY3156 and NY3157, respectively). To analyze Sec2p localization in the *ypt31*Δ *ypt32*^{A141D} sensitized background additionally deleted or not with the *YCK2* gene, the pRS305 Sec2C-3xGFP yeast integrating vector (NRB1416) was linearized using *Nsi*1 and transformed into NY3039 or NY3141 at the *SEC2* locus (NY3158 and NY3159). To analyze Sec15p localization, the pRS303 Sec15C-3xGFP yeast integrating vector (NRB1458) was linearized using SexA1 and transformed into the control yeast strain or the *yck-ts* mutant at the *SEC15* locus (NY3160 and NY3161, respectively). To analyze Ypt32p localization, the pRS306 ADHp GFP Ypt32 yeast integrating vector (NRB1325) was linearized using *Stu*1 and transformed into the control yeast strain or the *yck-ts* mutant at the *URA3* locus (NY3162 and NY3163, respectively). The expression of all fusion proteins was confirmed by Western blot analysis.

To analyze the effect of phosphomutations in *SEC2* on Bgl2p secretion, the pRS305 Sec2C-3xGFP WT, S181-8A or D/E yeast integrating vectors (NRB1416, NRB1506, and NRB1507, respectively) were linearized using *Nsi*1 and transformed into control yeast strain and *yck-ts* mutant (NY3109 and NY3110, respectively) at the *SEC2* locus (NY3169, NY3170,NY3171, NY3178, and NY3179).

The strain deleted for the *YCK2* gene, used for the genetic interaction screen (NY3140), was generated as described in Longtine *et al.* (1998). The deletion of the *YCK2* gene was confirmed by PCR analysis. This mutant strain was then crossed to different mutant strains affected in components of the secretory pathway.

For the genetic interaction screen with the nonphosphorylatable Sec2p mutant, the control and mutant strains (NY2911 and NY3037, respectively), both having Sec2p tagged with 3xGFP, were crossed to different mutant strains affected in components of the secretory pathway.

Sec2p mobility shift analysis

Yeast cells overexpressing Sec2p (full-length or 1–508) on a CEN vector were lysed at early log phase by NaOH treatment (5-min incubation with 0.1 M NaOH and pellets were directly resuspended with sample buffer). Lysates were separated by SDS–PAGE (8%) and analyzed with anti-Sec2p polyclonal antibody (laboratory antibody, 1:1000 dilution) as the primary antibody. Horseradish peroxidase (HRP)–conjugated goat anti-rabbit immunoglobulin G (IgG; 1:10,000 dilution) was used as the secondary antibody and detected with Pierce ECL Western Blotting Substrate (Thermo Scientific, Waltham, MA).

In Figure 1B, D, and E, top, Sec2p was purified from yeast as described in Stalder *et al.* (2013). For CIP treatment, the beads were washed three times with 0.5 ml of NEB buffer 3 and incubated with CIP for 20 min at 37°C (5 µl of CIP enzyme 10,000 U/ml [New England Biolabs, Ipswich, MA] into 100 µl of a 50% slurry of beads). For the condition CIP and EDTA, 50 mM EDTA was added in addition to CIP. Sec2p mobility was then analyzed by SDS–PAGE (8%) with Sec2p antibody as described or directly by Coomassie brilliant blue staining after SDS–PAGE (6%).

Expression and purification of GST Sec2p from *E. coli*

GST alone or the different truncated or mutated GST-Sec2 alleles in pGEX4T1 vectors (NRB1152, NRB1428, NRB1431, NRB1432, NRB1498, and NRB1499) were transformed into *E. coli* Bl21 cells. The expression and the purification of the corresponding proteins were performed as previously described (Stalder *et al.*, 2013; Stalder and Novick, 2015). The proteins bound to glutathione–Sepharose beads were used the next day for in vitro binding experiments.

For in vitro kinase assays and nucleotide exchange assays, GST-Sec2p 1-508 or full-length WT, S181-8A, or D/E was eluted with a buffer containing 100 mM Tris, pH 8.0, 300 mM NaCl, and 20 mM glutathione. Glutathione was then removed by dialysis against 20 mM Tris, pH 7.5, 100 mM NaCl, 1 mM $MgCl_2$, 1 mM dithiothreitol (DTT), and 10% glycerol. For nucleotide exchange assays, Sec2p was concentrated to ~10 µM. Proteins were stored at −80°C. The concentration of purified protein was determined by SDS–PAGE with bovine serum albumin (BSA) as standard.

Expression and purification of hexahistidine-tagged Sec4p from *E. coli*

NRB639 was transformed into *E. coli* Bl21 cells. Cells were grown at 37°C to an OD_{600} of 0.6 and induced using 0.1 mM isopropyl β-D-1-thiogalactopyranoside overnight at 16°C. The bacterial pellet was resuspended in 1× phosphate-buffered saline (PBS), 160 mM NaCl, 15 mM imidazole, pH 8, 1 mM $MgCl_2$, 1 mM phenylmethylsulfonyl fluoride (PMSF), and protease inhibitors (Complete EDTA-free protease inhibitor cocktail tablets [Roche, Indianapolis, IN]). Cells were disrupted by sonication, and Triton X-100 was added to the suspension to a final concentration of 1%, followed by a 15-min incubation at 4°C. The suspension was then cleared by centrifugation (15,000 rpm for 30 min at 4°C). After 2 h of incubation with Ni^{2+}-nitriloacetic acid resin (Qiagen, Redwood City, CA), the beads were washed with 1× PBS, 160 mM NaCl, 25 mM imidazole, pH 8, 1 mM $MgCl_2$, and 0.1% Triton X-100. Hexahistidine (His_6)-Sec4p was eluted with a buffer containing 1× PBS, 160 mM NaCl, 300 mM imidazole, and 1 mM $MgCl_2$. Imidazole was then removed by an overnight dialysis against 20 mM Tris, pH 7.2, 100 mM NaCl, 1 mM $MgCl_2$, 1 mM DTT, and 100 µM GDP.

To load His_6-Sec4p with GDP, $MgCl_2$ was removed by using a PD-10 column (GE Healthcare, Piscataway, NJ) and a buffer containing 50 mM Tris, pH 8, 100 mM KCl, and 1 mM DTT. Then 1 mM EDTA and 1 mM GDP were added to His_6-Sec4p, and the reaction was incubated for 30 min at room temperature. To terminate the loading reaction, $MgCl_2$ was added to a final concentration of 20 mM. The excess GDP was removed using a PD-10 column and a buffer containing 20 mM Tris, pH 7.5, 100 mM NaCl, 1 mM $MgCl_2$, 10% glycerol, and 1 mM DTT. His_6-Sec4p was directly stored at −80°C. The concentration of His_6-Sec4p was determined by SDS–PAGE with BSA as standard.

In vitro binding assay

Yeast cells overexpressing GFP-Yck2p (NY3138) were resuspended in lysis buffer containing 1× PBS, 1 mM $MgCl_2$, 1 mM PMSF, protease inhibitors (Complete EDTA-free protease inhibitor cocktail tablets), and 5 mM DTT. Cells were disrupted in a bead beater using 0.5-mm zirconia/silica beads. Triton X-100 was added to the lysate to a final concentration of 1%, followed by a 15-min incubation at 4°C and finally clearance by centrifugation at 13,000 rpm for 20 min.

One hundred OD_{595} units of yeast lysate were incubated with 0.2 µM GST-Sec2p protein purified from bacteria and immobilized on glutathione–Sepharose beads. After 2 h of incubation at 4°C, the beads were washed quickly three times with 1 ml of a buffer containing 1× PBS, 5 mM $MgCl_2$, 0.05% Triton X-100, and 1 mM DTT.

Bound products were separated by SDS–PAGE and analyzed with anti-GFP monoclonal antibody (1:1000 dilution; sc-9996; Santa Cruz Biotechnology, Santa Cruz, CA) as the primary antibody. The amount of GST-Sec2p in the reaction was verified by Western blotting with anti-GST antibody (1:1000 dilution; sc-459; Santa Cruz Biotechnology). HRP-conjugated goat anti-mouse and anti-rabbit IgG (1:10,000 dilution) were used, respectively, as the secondary antibodies and detected with Pierce ECL Western Blotting Substrate.

Liposome preparation

1-Palmitoyl-2-oleoyl-*sn*-glycero-3-phospho-L-serine (POPS), 1,2-dipalmitoyl-*sn*-glycero-3-phosphoethanolamine (DPPE), 1,2-dipalmitoyl-*sn*-glycero-3-phosphocholine (DPPC), and brain L-α-PI(4)P were from Avanti Polar Lipids (Alabaster, AL). All liposomes contained 20 mol% DPPE and 30 mol% POPS, with or without 2, 5, or 10 mol% PI(4)P, and the remaining lipid was DPPC. Lipids in chloroform were mixed in a pear-shaped glass container. The glass container was attached to a rotary evaporator and immersed in a water bath at 33°C for 5 min before evaporation. A lipid film was produced by rapid evaporation of chloroform under vacuum. The lipid film was resuspended in 50 mM 4-(2-hydroxyethyl)-1-piperazineethanesulfonic acid (HEPES) and 120 mM KAc, pH 7.2 (4 mM lipids). The resuspension was submitted to five cycles of freezing and thawing and extruded through a polycarbonate filter with a pore size of 0.1 µm.

In vitro kinase assay

Yeast lysates overexpressing GFP-Yck2p WT (NY3138) or H187Y (NY3139) were prepared as described for the in vitro binding assay, except that the lysis buffer was the following: 50 mM Tris, pH 7.5, 150 mM NaCl, 1 mM $MgCl_2$, 1 mM PMSF, and protease inhibitors (Complete EDTA-free protease inhibitor cocktail tablets).

A 2-mg amount of lysates (in a final volume of 1 ml of lysis buffer) was precleared with 10 µl of protein A/G beads (Thermo Scientific) for 45 min at 4°C. GFP-Yck2p was immunoprecipitated for 2 h at 4°C with anti-GFP polyclonal antibody (gift from the Ferro-Novick lab). A 20-µl of protein A/G beads was added and incubated for 1½ h at 4°C. Beads were washed three times with 1 ml of lysis buffer and twice with 1 ml of kinase assay buffer containing 50 mM HEPES, pH 7.4, 5 mM $MgCl_2$, and 1 mM DTT. Beads were incubated in a final volume of 30 µl of kinase assay buffer complemented with 2 µg of eluted bacterial GST-Sec2p 1-508 WT or S181-8A (0.81 µM) with or without 0.81 mM liposomes. After 5 min of incubation at 37°C, 5 mM ATP was added or not, and the reaction was incubated for an additional 1 h at 37°C.

Samples were separated by SDS–PAGE (8%), and GST Sec2p 1-508 phosphorylation was analyzed with anti-GST antibody (1:1000 dilution; sc-459; Santa Cruz Biotechnology), and GFP-Yck2p amount with anti-GFP monoclonal antibody (1:1000 dilution; sc-9996; Santa Cruz Biotechnology). HRP-conjugated goat anti-rabbit and anti-mouse IgG (1:10,000 dilution) were used, respectively, as the secondary antibodies and detected with Pierce ECL Western Blotting Substrate.

Sec2p–Sec15p coimmunoprecipitation assay

Yeast cells were grown overnight to early log phase in yeast extract/peptone/dextrose (YPD) medium at 25°C and shifted for 1 h to 37°C (NY3134, NY3135, NY3136, and NY3137). The Sec2p–Sec15p coimmunoprecipitation assay was performed as described in Stalder and Novick (2015), except that the lysis buffer was complemented with phosphatase inhibitors (PhosSTOP tablets [Roche]) and that the incubation of the lysates with anti-GFP antibody was performed for 2 h instead of overnight.

Nucleotide exchange assays

Nucleotide exchange on His_6-Sec4p was monitored by following the fluorescence signal created by a FRET interaction between His_6-Sec4p and a fluorescent analogue of GTP, mant-GTP (AnaSpec, Fremont, CA). Experiments were performed at 15°C in a buffer containing 50 mM HEPES, pH 7.2, 120 mM potassium acetate, 1 mM $MgCl_2$, and 1 mM DTT (final volume of 500 µl). Fluorescence emission was monitored by using a fluorimeter (Fluorolog [Horiba Scientific, Edison, NJ]) with the following settings: excitation, 290 nm; emission, 460 nm; intermediate slit, 2 nm. At 60 s, 1 µM of GDP-loaded full-length His_6-Sec4p protein was added to the reaction; at 120 s, 40 µM mant-GTP; and at 180 s, 20 or 100 nM full-length GST-Sec2p WT, S181-A, or S181-8D/E.

Growth test

Cells were grown overnight in YPD medium at 25°C. Cells were diluted to an OD_{600} of 0.04 and spotted in fivefold serial dilution on YPD plates, which were incubated at different temperatures.

Bgl2p secretion assay

Control, *yck-ts* mutant, and *sec6-4* yeast strains (NY3109, NY3110, and NY17, respectively) were grown overnight to early log phase at 25°C in YPD medium and shifted for 1½ h at 32°C. Five OD_{600} units were collected and washed with 10 mM NaN_3 and 1.2 M sorbitol. After 10 min of incubation on ice, cells were resuspended with 1% 2-mercaptoethanol in 50 mM Tris, pH 8.0, and 10 mM NaN_3 and incubated for another 15 min on ice. Cells were spheroplasted with 1 ml of potassium phosphate buffer (pH 7.5) containing 1.2 M sorbitol, 1 mM $MgCl_2$, 10 mM NaN_3, and 150 µg/ml Zymolyase 100T (Nacalai Tesque, San Diego, CA) for 45 min at 37°C with gentle shaking. Spheroplasts were then pelleted at 5000 g for 10 min, and 100 µl of the supernatant (external pool) was mixed with 20 µl of 4× SDS sample buffer. The pellet (internal pool) was resuspended in 100 µl of 2× SDS sample buffer. A 2.5% amount of the internal pool and 0.25% of the external pool were separated by SDS–PAGE (12%) and analyzed by Western blotting with anti-Bgl2p antibody (1:10,000 dilution; a gift from the laboratory of Randy Schekman, University of California, Berkeley, CA). HRP-conjugated goat anti-rabbit IgG (1:10,000 dilution) was used as the secondary antibody and was detected with Pierce ECL Western Blotting Substrate.

Fluorescence microscopy

GFP visualization was performed as described in Stalder *et al*. (2013).

Electron microscopy

WT and *yck-ts* mutant strains (NY3109 and NY3110, respectively) were grown overnight to early log phase at 25°C in YPD medium, shifted for 2 h at 37°C, and processed for electron microscopy as described by Chen *et al*. (2012), except that samples were embedded in a Durcupan resin instead of a Spurr resin.

ACKNOWLEDGMENTS

We thank Lucy Robinson for the generous gift of yeast strains, plasmids, and protocols, Christian Ungermann for helpful comments, Susan Ferro-Novick and her laboratory for helpful discussions and the gift of antibodies and protocols, Deepali Bhandari for helpful discussions, Ying Jones from M. Farquhar's laboratory for the preparation of samples for electron microscopy, Stephen Adams from R. Tsien's laboratory for help with the fluorimeter, S. Dowdy's laboratory for help with the rotary evaporator, R. Schekman's laboratory for the Bgl2p antibody, F. Luca's laboratory for yeast strains, Julie Yuan from

P. Novick's laboratory for her help with growth tests, and P. Novick's laboratory for plasmids, reagents. and protocols. This study was supported by National Institutes of Health Grant GM082861 to P.J.N.

REFERENCES

Babu P, Bryan JD, Panek HR, Jordan SL, Forbrich BM, Kelley SC, Colvin RT, Robinson LC (2002). Plasma membrane localization of the Yck2p yeast casein kinase 1 isoform requires the C-terminal extension and secretory pathway function. J Cell Sci 115, 4957–4968.

Baird D, Stefan C, Audhya A, Weys S, Emr SD (2008). Assembly of the PtdIns 4-kinase Stt4 complex at the plasma membrane requires Ypp1 and Efr3. J Cell Biol 183, 1061–1074.

Bishop A, Lane R, Beniston R, Chapa-y-Lazo B, Smythe C, Sudbery P (2010). Hyphal growth in Candida albicans requires the phosphorylation of Sec2 by the Cdc28-Ccn1/Hgc1 kinase. EMBO J 29, 2930–2942.

Cabrera M, Langemeyer L, Mari M, Rethmeier R, Orban I, Perz A, Bröcker C, Griffith J, Klose D, Steinhoff HJ, *et al.* (2010). Phosphorylation of a membrane curvature-sensing motif switches function of the HOPS subunit Vps41 in membrane tethering. J Cell Biol 191, 845–859.

Chen S, Novick P, Ferro-Novick S (2012). ER network formation requires a balance of the dynamin-like GTPase Sey1p and the Lunapark family member Lnp1p. Nat Cell Biol 14, 707–716.

Chiba S, Amagai Y, Homma Y, Fukuda M, Mizuno K (2013). NDR2-mediated Rabin8 phosphorylation is crucial for ciliogenesis by switching binding specificity from phosphatidylserine to Sec15. EMBO J 32, 874–885.

Demmel L, Beck M, Klose C, Schlaitz AL, Gloor Y, Hsu PP, Havlis J, Shevchenko A, Krause E, Kalaidzidis Y, *et al.* (2008). Nucleocytoplasmic shuttling of the Golgi phosphatidylinositol 4-kinase Pik1 is regulated by 14-3-3 proteins and coordinates Golgi function with cell growth. Mol Biol Cell 19, 1046–1061.

Donovan KW, Bretscher A (2015). Tracking individual secretory vesicles during exocytosis reveals an ordered and regulated process. J Cell Biol 210, 181–189.

Elkind NB, Walch-Solimena C, Novick PJ (2000). The role of the COOH terminus of Sec2p in the transport of post-Golgi vesicles. J Cell Biol 149, 95–110.

Estrada E, Agostinis P, Vandenheede JR, Goris J, Merlevede W, François J, Goffeau A, Ghislain M (1996). Phosphorylation of yeast plasma membrane H+-ATPase by casein kinase I. J Biol Chem 271, 32064–32072.

Gadura N, Robinson LC, Michels CA (2006). Glc7-Reg1 phosphatase signals to Yck1,2 casein kinase 1 to regulate transport activity and glucose-induced inactivation of Saccharomyces maltose permease. Genetics 172, 1427–1439.

Gault WJ, Olguin P, Weber U, Mlodzik M (2012). Drosophila CK1-γ, gilgamesh, controls PCP-mediated morphogenesis through regulation of vesicle trafficking. J Cell Biol 196, 605–621.

Grosshans BL, Andreeva A, Gangar A, Niessen S, Yates JR, Brennwald P, Novick P (2006). The yeast lgl family member Sro7p is an effector of the secretory Rab GTPase Sec4p. J Cell Biol 172, 55–66.

Guo W, Roth D, Walch-Solimena C, Novick P (1999). The exocyst is an effector for Sec4p, targeting secretory vesicles to sites of exocytosis. EMBO J 18, 1071–1080.

Hergovich A, Stegert MR, Schmitz D, Hemmings Ba (2006). NDR kinases regulate essential cell processes from yeast to humans. Nat Rev Mol Cell Biol 7, 253–264.

Hutagalung AH, Novick PJ (2011). Role of Rab GTPases in membrane traffic and cell physiology. Physiol Rev 91, 119–149.

Jin Y, Sultana A, Gandhi P, Franklin E, Hamamoto S, Khan AR, Munson M, Schekman R, Weisman LS (2011). Myosin V transports secretory vesicles via a Rab GTPase cascade and interaction with the exocyst complex. Dev Cell 21, 1156–1170.

Kurischko C, Kuravi VK, Wannissorn N, Nazarov PA, Husain M, Zhang C, Shokat KM, McCaffery JM, Luca FC (2008). The yeast LATS/Ndr kinase Cbk1 regulates growth via Golgi-dependent glycosylation and secretion. Mol Biol Cell 19, 5559–5578.

Lawrence G, Brown CC, Flood BA, Karunakaran S, Cabrera M, Nordmann M, Ungermann C, Fratti RA (2014). Dynamic association of the PI3P-interacting Mon1-Ccz1 GEF with vacuoles is controlled through its phosphorylation by the type 1 casein kinase Yck3. Mol Biol Cell 25, 1608–1619.

Ling Y, Hayano S, Novick P (2014). Osh4p is needed to reduce the level of phosphatidylinositol-4-phosphate on secretory vesicles as they mature. Mol Biol Cell 25, 3389–3400.

Longtine MS, McKenzie A, Demarini DJ, Shah NG, Wach A, Brachat A, Philippsen P, Pringle JR (1998). Additional modules for versatile and economical PCR-based gene deletion and modification in Saccharomyces cerevisiae. Yeast 14, 953–961.

Lord C, Bhandari D, Menon S, Ghassemian M, Nycz D, Hay J, Ghosh P, Ferro-Novick S (2011). Sequential interactions with Sec23 control the direction of vesicle traffic. Nature 473, 181–186.

Marchal C, Dupré S, Urban-Grimal D (2002). Casein kinase I controls a late step in the endocytic trafficking of yeast uracil permease. J Cell Sci 115, 217–226.

Mazanka E, Alexander J, Yeh BJ, Charoenpong P, Lowery DM, Yaffe M, Weiss EL (2008). The NDR/LATS family kinase Cbk1 directly controls transcriptional asymmetry. PLoS Biol 6, e203.

Medkova M, France YE, Coleman J, Novick P (2006). The rab exchange factor Sec2p reversibly associates with the exocyst. Mol Biol Cell 17, 2757–2769.

Mizuno-Yamasaki E, Medkova M, Coleman J, Novick P (2010). Phosphatidylinositol 4-phosphate controls both membrane recruitment and a regulatory switch of the Rab GEF Sec2p. Dev Cell 18, 828–840.

Mizuno-Yamasaki E, Rivera-Molina F, Novick P (2012). GTPase networks in membrane traffic. Annu Rev Biochem 81, 637–659.

Mochida K, Ohsumi Y, Nakatogawa H (2014). Hrr25 phosphorylates the autophagic receptor Atg34 to promote vacuolar transport of α-mannosidase under nitrogen starvation conditions. FEBS Lett 588, 3862–3869.

Moriya H, Johnston M (2004). Glucose sensing and signaling in Saccharomyces cerevisiae through the Rgt2 glucose sensor and casein kinase I. Proc Natl Acad Sci USA 101, 1572–1577.

Ortiz D, Medkova M, Walch-Solimena C, Novick P (2002). Ypt32 recruits the Sec4p guanine nucleotide exchange factor, Sec2p, to secretory vesicles; evidence for a Rab cascade in yeast. J Cell Biol 157, 1005.

Panek HR, Stepp JD, Engle HM, Marks KM, Tan PK, Lemmon SK, Robinson LC (1997). Suppressors of YCK-encoded yeast casein kinase 1 deficiency define the four subunits of a novel clathrin AP-like complex. EMBO J 16, 4194–4204.

Pfaffenwimmer T, Reiter W, Brach T, Nogellova VN, Papinski D, Schuschnig M, Abert C, Ammerer G, Martens S, Kraft C (2014). Hrr 25 kinase promotes selective autophagy by phosphorylating the cargo receptor Atg19. EMBO Rep 15, 862–870.

Ptacek J, Devgan G, Michaud G, Zhu H, Zhu X, Fasolo J, Guo H, Jona G, Breitkreutz A, Sopko R, *et al.* (2005). Global analysis of protein phosphorylation in yeast. Nature 438, 679–684.

Robinson L, Menold M, Garrett S, Culbertson M (1993). Casein kinase I-like protein kinases encoded by YCKJ and YCK2 are required for yeast morphogenesis. Mol Cell Biol 13, 2870–2881.

Stalder D, Mizuno-Yamasaki E, Ghassemian M, Novick PJ (2013). Phosphorylation of the Rab exchange factor Sec2p directs a switch in regulatory binding partners. Proc Natl Acad Sci USA 110, 19995–20002.

Stalder D, Novick PJ (2015). Rab GTPases. Methods Mol Biol 1298, 85–98.

Stock SD, Hama H, DeWald DB, Takemoto JY (1999). SEC14-dependent secretion in Saccharomyces cerevisiae. J Biol Chem 274, 12979–12983.

Tanaka C, Tan L-J, Mochida K, Kirisako H, Koizumi M, Asai E, Sakoh-Nakatogawa M, Ohsumi Y, Nakatogawa H (2014). Hrr25 triggers selective autophagy-related pathways by phosphorylating receptor proteins. J Cell Biol 207, 91–105.

Ultanir SK, Hertz NT, Li G, Ge WP, Burlingame AL, Pleasure SJ, Shokat KM, Jan LY, Jan YN (2012). Chemical genetic identification of NDR1/2 kinase substrates AAK1 and Rabin8 Uncovers their roles in dendrite arborization and spine development. Neuron 73, 1127–1142.

Vancura A, Sessler A, Leichus B, Kuret J (1994). A prenylation motif is required for plasma membrane localization and biochemical function of casein kinase I in budding yeast. J Biol Chem 269, 19271–19278.

Walch-Solimena C, Collins RN, Novick PJ (1997). Sec2p mediates nucleotide exchange on Sec4p and is involved in polarized delivery of post-Golgi vesicles. J Cell Biol 137, 1495–1509.

Wang J, Davis S, Menon S, Zhang J, Ding J, Cervantes S, Miller E, Jiang Y, Ferro-Novick S (2015a). Ypt1/Rab1 regulates Hrr25/CK1 kinase activity in ER-Golgi traffic and macroautophagy. J Cell Biol 210, 273–285.

Wang J, Ren J, Wu B, Feng S, Cai G, Tuluc F, Peränen J, Guo W (2015b). Activation of Rab8 guanine nucleotide exchange factor Rabin8 by ERK1/2 in response to EGF signaling. Proc Natl Acad Sci USA 112, 148–153.

Zhai L, Graves PR, Robinson LC, Italiano M, Culbertson MR, Rowles J, Cobb MH, DePaoli-Roach AA, Roach PJ (1995). Casein kinase I gamma subfamily. Molecular cloning, expression, and characterization of three mammalian isoforms and complementation of defects in the Saccharomyces cerevisiae YCK ganes. J Biol Chem 270, 12717–12724.

Zick M, Wickner W (2012). Phosphorylation of the effector complex HOPS by the vacuolar kinase Yck3p confers Rab nucleotide specificity for vacuole docking and fusion. Mol Biol Cell 23, 3429–3437.